Schweizerische Eidgenossenschaft
Confédération suisse
Confederazione Svizzera
Confederaziun svizra

Eidgenössisches Departement für
Umwelt, Verkehr, Energie und Kommunikation UVEK

Bundesamt für Energie BFE

Final report 07.12.2015

Solar Production of Zinc and Hydrogen – 100 kW Solar Pilot Reactor for ZnO Dissociation

Contracting body:

Swiss Federal Office of Energy SFOE
Research Programme Industrielle Solarenergienutzung
CH-3003 Bern
www.bfe.admin.ch

Contractor:

Paul Scherrer Institut
Labor für Solartechnik
CH-5232 Villigen PSI
www.psi.ch ; http://www.psi.ch/lst/

Author:

Anton Meier, Paul Scherrer Institut, anton.meier@psi.ch
Erik Koepf, Paul Scherrer Institut

SFOE Head of domain: Stefan Oberholzer
SFOE Contract number: SI/500403-01

Content

Project goals

Background – This Final Report covers the achievements of the P&D project *Solar Production of Zinc and Hydrogen – 100 kW Solar Pilot Reactor for ZnO Dissociation* (2013-2015) [1], which is a follow-up of the P&D project *Towards Industrial Solar Production of Zinc and Hydrogen – 100 kW Solar Pilot Reactor for ZnO Dissociation* (2010-2013) [2],[3] and closely related to the R&D project *Solar Production of Zinc and Hydrogen – Reactor Optimisation for Scale-Up* (2008-11) [4].

Introduction – The solar two-step Zn/ZnO redox cycle [5] consists of: (1) the endothermic dissociation of ZnO to Zn and O_2 at 2000 K using concentrated solar energy; and (2) the exothermic reaction of Zn with H_2O/CO_2 to H_2/CO (mixture known as *syngas*, the precursor of liquid hydrocarbon fuels) and the initial ZnO; the latter is recycled to the first step, thus closing the material cycle. Following the technical demonstration with a 10 kW_{th} solar reactor prototype, a 100 kW_{th} solar pilot plant has been designed, fabricated, and experimentally tested at the large-scale solar concentrating facility of PROMES-CNRS in Odeillo, France. The operational experience of two previous experimental campaigns in 2011 and 2012 points out to further R&D needs and guides the development of an industrial solar chemical plant for the production of H_2, syngas, and liquid hydrocarbon fuels.

Research purpose – The main purpose of the current research project is to optimize the solar reactor technology for the thermal dissociation of ZnO and to successfully demonstrate the fully integrated reactor at pilot scale (solar power input of 100 kW_{th}). An advanced numerical heat transfer model of the 100 kW_{th} solar reactor will be developed and validated with experimental data from the test campaigns at the 1 MW Solar Furnace (MWSF) in Odeillo, France. Towards the end of this P&D project, conceptual designs and preliminary economics for commercial solar Zn production and storage facilities will be developed based on large-scale concentrating solar power (CSP) tower technology.

The results from this research program will advance our ability to store solar energy as a fuel, such as Zn, H_2, or syngas in a manner that increases our chances of having a sustainable solution to the current world problem of being dependent on a limited supply of fossil fuels.

Project status description – The main project achievements are briefly summarized:

- Until end of 2013, the 100 kW_{th} solar pilot reactor and peripheral equipment – used in the experimental campaign 2012 – has been repaired, modified, optimized, and re-assembled.
- In January/February 2014, the solar reactor has been installed and commissioned in *PSI*'s High-Flux Solar Simulator (HFSS).
- Between March and July 2014, an extensive measurement campaign at temperatures up to 1300°C has been performed at the HFSS. The main tasks included
    - Functional tests of all reactor and peripheral components at elevated temperatures
    - Verification of functionality of process control program; systems checks
    - High temperature flow visualization and aerodynamic window protection
- The 3rd experimental campaign at the MWSF in Odeillo, France, was conducted between August 25 and October 30, 2014:
    - Week 0 (25.08.-01.09.): Pilot plant transport to Odeillo; Installation in Solar Tower (PSI staff); Heliostat calibration (PROMES-CNRS staff)
    - Weeks 1-4 (02.09.-26.09.): Experimental campaign (financed by EU project SFERA2)
    - Weeks 5-8 (29.09.-24.10.): Experimental campaign (financed by BFE/PSI)
    - Week 9 (25.-30.10.): Pilot plant dismounting and transport back to PSI
- Final project steps November 2014 and December 2015 (pending publications early 2016):
    - Data analysis and performance evaluation of the 3rd test campaign at the MWSF
    - Validation of the numerical heat transfer model of the 100 kW_{th} solar reactor
    - Development of the conceptual design and economic analysis of a first-of-its-kind industrial demonstration plant for the production of zinc (10-50 MW_{th})
    - Publications of results related to the 3rd test campaign (2015/16)
    - Publications on window protection (2015/16) and techno-economic analysis (2016)
    - Detailed technical assessment of the 100 kW_{th} solar reactor pilot plant (2016)

Project status evaluation – In the following, the project status is presented in more detail, with emphasis on high temperature flow visualization and aerodynamic window protection.

Completed tasks and achieved results

The major achievements are described according to the project specification defined in the proposal [1], which encompasses four work packages (WPs) with objectives, description of work, deliverables and milestones. Note that the work performed in WP1 (“Optimization of Solar Reactor Technology”) and WP2 (“Solar Pilot Plant Testing at High-Flux Solar Simulator (HFSS) of PSI”) has already been reported in the Annual Report 2013 [6] and in the Intermediate Report 2014 [7], as well as in a peer-reviewed journal paper [8] and at the SolarPACES Conference 2014 [9]. The work conducted in WP3 (“Solar Pilot Plant Experimental Demonstration at MWSF of PROMES-CNRS in Odeillo”) has been reported at the SolarPACES Conference 2015 [16], and a comprehensive summary paper is under review. From the work of WP4 (“Modeling, Conceptual Design and Economic Assessment”), one modeling paper has been published and two more papers are in preparation.

WP1:
Optimization of Solar Reactor Technology

Objectives – Repair, modification, and optimization of the 100 kW_{th} solar reactor for ZnO dissociation.

Solar reactor design – A complete description of the reactor can be found in [8]. The receiver-reactor is designed to operate at a nominal thermal power of 100 kW provided by concentrated solar radiation that is horizontally incident, and effect the thermochemical dissociation of ZnO into metallic Zn. The reactor is closed from atmosphere by a transparent quartz window, through which concentrated solar radiation can enter. From the window diameter, the frustum of the reactor converges to the aperture, which then connects to the reaction cavity. The reactor can operate semi-continuously while solar radiation is available to heat the reaction cavity, and ZnO reactant powder is fed via a screw-feeding apparatus that enters the reaction cavity from the back while the entire reactor rotates relative to the angularly-fixed feeder; ZnO powder is dispersed evenly on the reaction surface during a single feed-cycle. As the reaction proceeds, Zn vapor evolves from the reaction surface and is swept by an auxiliary flow of inert gas into the quench device where the stream is rapidly cooled and the Zn vapor is condensed. Solid Zn particles are then filtered from the flow downstream. Figure 1 depicts a three-quarter section view of the reactor where the view angles of the infrared (IR) and visual cameras are shown, along with a cross section view where relevant features of the reactor are labeled. The reactor window is 12 mm thick quartz (TCS-3, Heraeus Quarzglas, Germany) and 600 mm in diameter. Critical areas of the reactor are water-cooled in order to maintain material stability during operation, including: the screw feeder, quench unit, quartz window mount, and frustum. The reactor shell is made of aluminum, housing a porous ceramic insulation followed by a layer of Al_2O_3 bricks whose interior surface defines the reaction cavity. Typically, a 1-2 cm thick layer of sintered ZnO coats the entire reaction cavity surface.

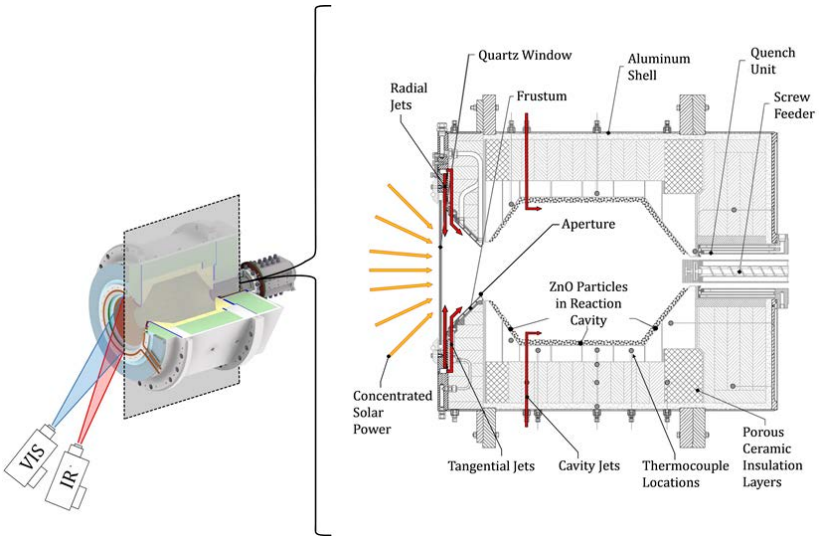

Figure 1: Three-quarter and cross section view of the receiver-reactor. Views of the visual (VIS) and infrared (IR) cameras are indicated, and relevant features of the reactor are labeled. From [9].

Description of Work – The status is summarized according to the Task structure of this WP. Besides the modifications of the window structure and the front cone coating (Tasks 1.2 and 1.3) implemented in 2013, additional solar reactor components have been modified or replaced.

Task 1.1: Solar reactor modification

a. Additional blower and frequency converter installed at reactor outlet for pressure control inside reactor cavity.
b. Over-pressure valves (mechanical and controlled by pressure sensor) installed.
c. New pressure sensors for off-gas controlling mounted.
d. Opening/closing mechanism of particle filters modified.

Task 1.4: Feeder modification

a. New design for feeder cap protection using Al_2O_3 insulation board.
b. New feeder-cap opening/closing mechanism tested.
c. New mixer and vibration motors for ZnO hopper (ZnO container) installed.

Task 1.5: Gas inlet modification

a. A modular nozzle system was incorporated for injecting inert gas (Ar) both for the aerodynamic protection of the window and for the efficient removal of the product gases, thus increasing the kinetics of the dissociation reaction.
b. The receiver-reactor was equipped with a set of 24 radial jets and 24 tangential jets located just next to the window plane (Fig. 2), and a set of six cavity jets oriented tangentially inside the reaction cavity.
c. Gas pre-heating of the cavity flow inside the Al_2O_3 pipes is enhanced by inserting ceramic Al_2O_3 foam. In contrast, preheating of radial and tangential window flows is not feasible due to water-cooled nozzle ring.

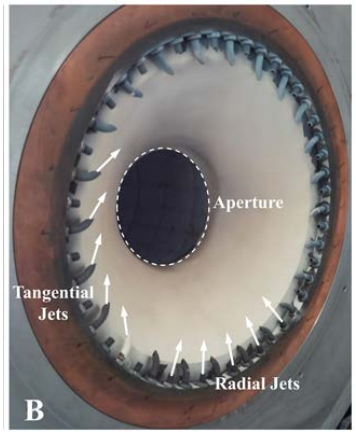

Figure 2: Modular nozzle system for injecting inert gas for aerodynamic window protection: With the reactor window dismounted, the aperture, frustum, and radial and tangential jets can be seen. From [9].

Task 1.6: Gas analysis modification

a. New off-gas sampling system installed.
b. Assessment of the gas analysis system (GC and Oxymat).

Miscellaneous:

a. A water-cooled radiation protection shield with a 600-mm-diameter opening for accepting concentrating solar radiation has been newly designed and fabricated at PSI. It will replace the leaking center part of the shield originally manufactured by PROMES-CNRS.
b. A movable camera box has been designed and is currently being fabricated. It will be mounted in front of the solar reactor at the MWSF in Odeillo. The IR and visible cameras will be used for high temperature flow visualization (see below).

Publication:

- Villasmil W., Brkic M., Wuillemin D., Meier A., Steinfeld A.: ***Pilot scale demonstration of a 100-kWth solar thermochemical plant for the thermal dissociation of ZnO***, ASME Journal of Solar Energy Engineering **136**, 011017-1/11, 2014. (**published paper attached**)

  Abstract – A solar-driven thermochemical pilot plant for the high-temperature thermal dissociation of ZnO has been designed, fabricated, and experimentally demonstrated. Tests were conducted at the large-scale solar concentrating facility of PROMES-CNRS by subjecting the solar reactor to concentrated radiative fluxes of up to 4477 suns and peak solar radiative power input of 140 kWth. The solar reactor was operated at temperatures up to 1936 K, yielding a Zn molar fraction of the condensed products in the range 12–49% that was largely dependent on the flow rate of Ar injected to quench the evolving gaseous products.

WP2:
Solar Pilot Plant Testing at High-Flux Solar Simulator (HFSS) of PSI

Objectives – Demonstration and evaluation of reliable rotary reactor operation at moderate temperatures in PSI's High-Flux Solar Simulator (HFSS), and determination of optimal gas flow configurations to prevent precipitations on front cone and window.

Experimental setup – The 100-kW_{th} solar thermochemical receiver-reactor was mounted at PSI's HFSS [10] atop a large, fixed steel frame and aligned with the focal axis of the light-cone produced by the solar simulator (Fig. 3). A carriage-assembly harnessing the reactor was equipped with wheels, allowing the reactor to roll in and out of the focal plane, while maintaining alignment with the solar simulator focal axis. The HFSS was operated at maximum power (~120 kW_{el}) for 10-15 hours during a typical experiment. A high-resolution visual camera (Nikon D5200, equipped with a 300-mm lens, ND3 filter, and an adjustable polarizing filter fixed to 80%) was mounted such that the front frustum section of the reactor could be visualized, and an IR camera (Hotfind-LXT, SDS® Infrared, temperature range -20°C–1500°C, FPA microbolometer, accuracy +/- 2%, resolution 384x288 pixels) was mounted such that the entire quartz window could be seen. Solar simulator operation, data acquisition, and gas flows were controlled online via computer interface from the control room located to the side of the experimental setup.

Figure 3 depicts a side view of the array of lamps, along with the position of the solar reactor. The focal height of the light cone is 2.54 m, which is aligned with the centerline of the reactor. The aperture of the reactor is aligned with the focal plane of the lamps in order to intercept maximum incident radiation. A plot of radiative intensity versus distance across the focal plane, acquired by imaging the light intensity on a water-cooled Lambertian target placed in the focal plane, can be seen in Fig. 3(A). Figure 3(B) depicts the flux map (the superimposed circle represents the aperture area) indicating solar radiation that is admitted into the cavity. In this case, 46.8 kW of thermal radiative power is delivered to the reactor cavity, and it is clear that as the reactor's aperture is 190 mm in diameter, nearly all of the radiative power provided by the HFSS is accepted into the reactor cavity.

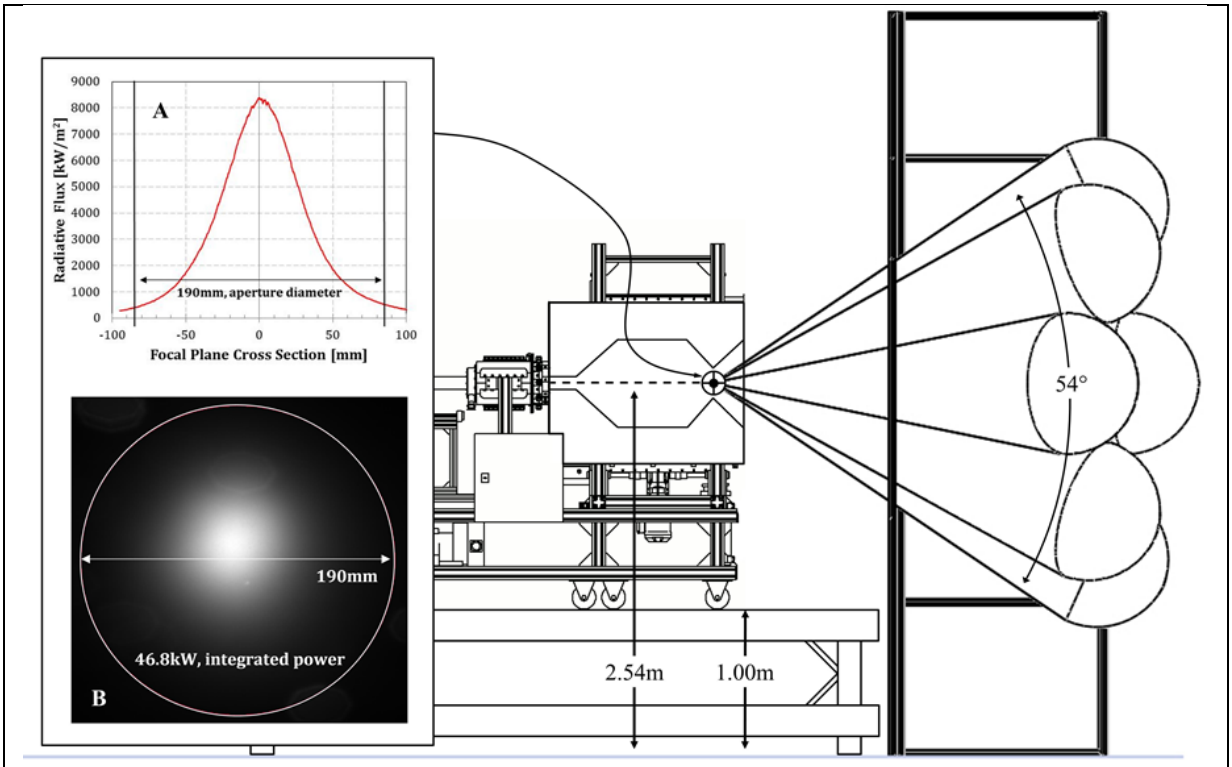

Figure 3: HFSS lamp orientation and relative position to receiver-reactor. The light-cone's vertical angle is shown as 54°, while the horizontal cone-angle (not shown) is 82°. A flux profile acquired from imaging of a Lambertian target aligned in the focal plane is also shown (A), along with a flux image indicating the integrated power inside the aperture area of the reactor (B). From [9].

Description of Work – The primary goal of the tests in the HFSS was to minimize the risks of operating the 100 kW_{th} solar thermochemical reactor under severe operating conditions using concentrated radiation. Besides functional tests of all components, the experimental work was focused on high temperature flow visualization for aerodynamic window protection. A Semester Thesis resulted from this work [11] and a paper was presented at the SolarPACES2014 Conference and published in a peer-reviewed Journal [9]. Here, the work performed in the HFSS is summarized according to the Task structure of this WP.

Task 2.1: Preparation work for 100 kW_{th} pilot plant tests at HFSS

a. In order to generate a rotating flow capable of protecting the quartz window from particle deposition, a set of tangential and radial jets are installed just next to the window plane in the frustum region of the reactor (see Fig. 1). A set of 24 tangential jets are installed circumferentially in the frustum, at a distance of 17 mm from the plane of the window. The tangential jet inner and outer diameter is 10 mm and 7 mm, respectively, and the nozzles are bent, rotated and installed such that their tangential and axial components are 64° and 10°, respectively. The nozzles are made of copper, and coated with Al_2O_3 spray paint to decrease their solar absorptance and protect them against high-flux radiation spillage. A set of 24 radial nozzles are installed circumferentially at a distance of 14 mm from the plane of the window; the nozzles and are comprised of brass with an outer and inner diameter of 10 mm and 8 mm, respectively. The window diameter exposed to incident solar radiation is 520 mm. The distance between the window plane and the aperture is 156 mm. The water-cooled frustum has an angle of 45° and is constructed of copper, coated with a layer of Al_2O_3. To minimize the background radiation of the hot cavity from the image of the visual camera, the camera is installed at an angle such that the cavity is just out of view (Fig. 1). This angle, $\theta_{vis} = 27°$, results in a reduction in visual depth of 30% along the centerline of the reactor, relative to the total distance between the window and aperture (156 mm). The IR camera is not affected by background radiation from the cavity because of the high absorptance of quartz glass to thermal radiation emitted below 1800°C. Thus, the camera is mounted parallel to the visual camera pointing at the center of the window.
b. Inside the reaction cavity, six nozzles composed of high-purity, fully-sintered Al_2O_3 are mounted at a distance of 345 mm from the window plane. The nozzles are installed with a 45° tangential component, and at a distance of 10 mm above the layer of sintered ZnO inside the reaction cavity. Injection of Ar through the cavity nozzles serves two purposes: (i) reduction of O_2 partial pressure at the reaction interface to enhance reaction kinetics [12], and (ii) tangential orientation of the gas injection adds rotational momentum to the flow of auxiliary gases originating in the frustum region, leading to increased flow stability. All reaction products and gases exit together at the rear of the reactor, where two 3-kW_{el}, side-channel blowers maintain a gauge pressure of 2 mbar in the cavity.
c. Auxiliary gas flows of Ar are delivered to the radial, tangential, and cavity jet lines via three mass flow controllers (MFC), with ranges 0-200 L_n/min, 0-200 L_n/min, and 0-500 L_n/min, respectively. As a flow-visualization aid, high purity CO (99.997% CO) is connected to a pulsing valve such that 0-2000 ms pulses of CO pressurized at 7.5 bar can be injected in-line with the Ar flowing through the cavity nozzles.

Task 2.2: Experimental campaign at HFSS

a. The reactor is designed to effect the thermal dissociation of ZnO at temperatures above 1750°C. With the power available from the HFSS, temperatures of 1350°C were achievable in the cavity after 8-10 hours of heating. To produce Zn in the reaction cavity at lower temperature, pulses of pure CO gas (0-2000 ms pulse, pressurized at 7.5 bar) were co-injected into the auxiliary cavity flow of Ar. The carbothermal reduction of ZnO into Zn, CO and CO_2 proceeds at temperatures above 1100°C. During experiments, short pulses of CO were used to seed the auxiliary flows with Zn in order to more effectively in-situ visualize the transport of product vapors by the auxiliary flows.
b. During an experiment, product Zn vapor and small aerosolized ZnO particles become entrained in the auxiliary inert gas flows of the reactor. Under various fluid dynamic conditions

controlled by varying the radial, tangential and cavity auxiliary flows of Ar, this particle laden flow can be driven into the frustum region of the reactor and towards the quartz window. As particles move into the frustum, they are directly illuminated by highly concentrated simulated solar radiation. These particles can then be directly visualized in-situ using a high-resolution, filtered CMOS digital camera. Images were taken with the camera set at a shutter speed of 1/1.6 s and aperture of f/5.6. Figure 4 depicts four images taken with the visual camera, where two types of useful visual data can be extracted: (i) direct identification of the flow pattern by means of visualizing the particles entrained in the gas, and (ii) assessment of the depositions developed on the quartz window while they are occurring. Additionally, an IR camera can assist in evaluating the depositions on the quartz window.

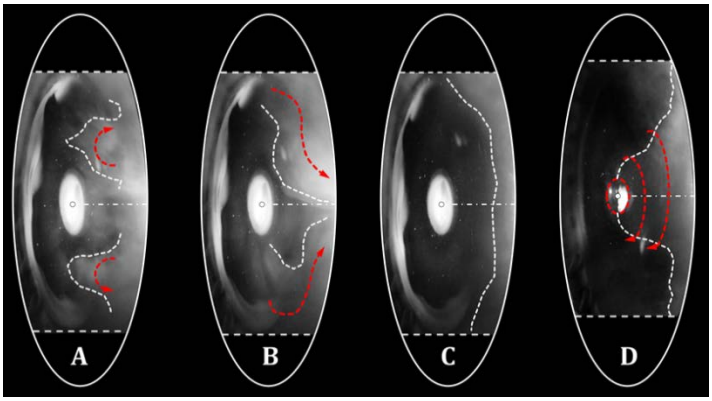

Figure 4: Images taken from the frustum region of the reactor using the visual camera: (A) A turbulent flow pattern is developed in the reactor, following by increased rotation which flushes out particles and stabilizes the flow (B). Particle migration to the window is completely suppressed (C), and with even further increased rotation, an updraft is formed and attached to the center of the window (D). From [9].

c. Images taken with the visual camera enabled accurate determination of the flow patterns inside the frustum region of the reactor. In Fig. 4(A) a highly turbulent flow is visible. In Fig. 4(B) and 4(C) the flow is stabilized and particles are removed from the frustum region. Figure 4(D) depicts an updraft of particles (similar to a tornado) that is in contact with the center of the window. The white spot in the center of all four images was formed by such an updraft of particles connected to the center of the window for a prolonged period of time. Images such as these were used to develop a metric to quantify the extent to which particles were in dangerous proximity of the window, thus increasing the likelihood of deposition on the window's surface. The so-called *severity scale* was introduced as a range between 0 and 4, with 0 representing no particles imaged in the frustum region of the reactor, and 4 representing a complete coverage of particles contacting the entirety of the window's inner surface. During experiments, the severity scale was used to quantify the developed flow pattern over a wide range of total auxiliary flow rates (Q_{tan}: 0-200 L_n/min; Q_{rad}: 0-200 L_n/min; Q_{cav}: 0-450 L_n/min).

Task 2.3: Performance evaluation

a. Severity of the threat to window contamination was assessed over a wide range of tangential, radial, and cavity flow rates. The influence of tangential flow rate on flow stability was found to be the most critical flow parameter. With insufficient rotational momentum imparted to the rotating flow by the tangential jets, turbulence would develop quickly in the frustum region of the reactor and immediately contaminate the quartz window. A contour plot of flow severity versus radial and tangential flow rates is presented in Fig. 5 for a fixed cavity flow rate of 400 L_n/min. The sharp transition from a deposition-free operating area (indicated by a severity of less than 2) to a condition of turbulent window deposition was found to be characteristic of the experimental setup. On the other hand, with increasing tangential flow rates, a stable but undesirable rotational flow pattern arises in the frustum region of the reactor. As a vortex flow is developed, originating from the tangential jets just inside the plane of the window, increasing rotation creates a low pressure core, which effectively pulls particle-laden gases from the cavity into the frustum region of the reactor and deposits them at the center of the window [13]. This can also be seen in Fig. 5, as increasing tangential flow increases the severity level, although not as sharply as and to a lesser degree than with decreasing tangential flow. For the fixed total cavity flow rate of 400 L_n/min, it is seen that a safe operating range falls between a total tangential flow rate of $95 < Q_{tan} < 135$ L_n/min and a total radial flow rate of $20 < Q_{rad} < 180$ L_n/min. Radial flow rate was found to have the less significant effect on flow severity.

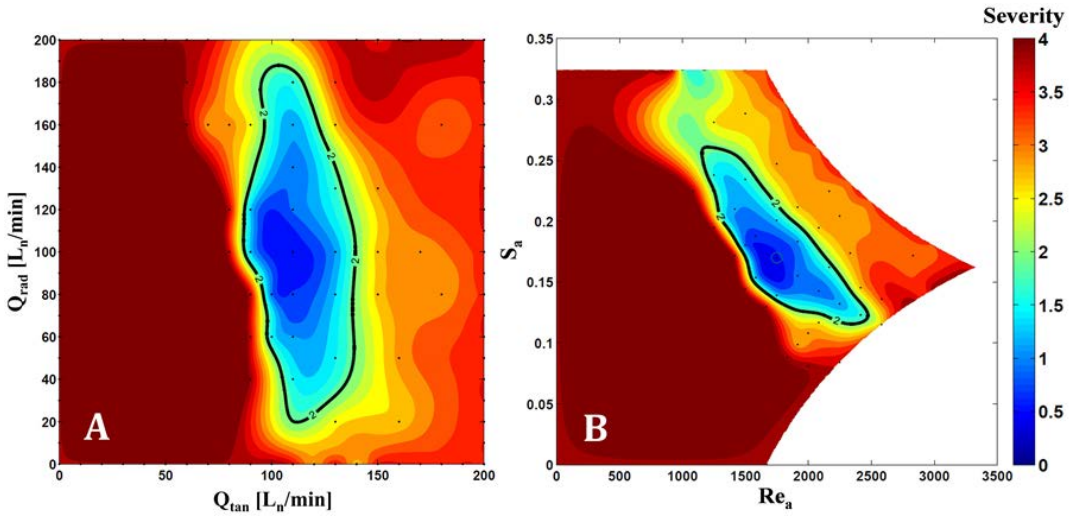

Figure 5: (A): Contour plot of severity level over the range of 0-200 L_n/min on the radial and tangential auxiliary gas flows, with the cavity flow fixed at 400 L_n/min. (B): Reynolds and swirl numbers defined at the aperture are also plotted for the same conditions. Regions below a severity level of 2 are indicated. From [9].

b. It is common to characterize rotating vortex flows by use of the non-dimensional swirl number. The swirl number defined at the tangential jet injection site, *S*, is defined below in Eq. 1, along with the swirl number at the aperture, S_a:

$$S = \frac{\Gamma\ r_0}{2\ Q\ h} = \frac{Q_{tan}\ cos\ \alpha}{Q_{tan}+Q_{rad}} \quad , \quad S_a = \frac{D_a}{D_w} S \tag{1}$$

where *α* is the tangential component of the tangential jets, Γ is the circulation of the swirling flow, r_0 is the hydraulic radius of the vortex core, *Q* is the total flow rate, and *h* is the height of the updraft. The swirl number at the aperture is derived from an inviscid flow approximation and thus scaled by the ratio of the aperture to window diameter, D_a/D_w [14]. The Reynolds number is also used to describe the auxiliary flow through the aperture of the reactor. Eq. 2 defines the Reynolds number and an approximation to the average gas velocity at the aperture:

$$Re_a = \frac{\rho\ u_a\ D_a}{\mu} \quad , \ with \quad u_a = \frac{4\ (Q_{rad}+Q_{tan})}{D_a^2\ \pi} \tag{2}$$

where ρ is the fluid density and μ is the dynamic viscosity. In this application, it is a valid assumption that the hydraulic diameter and aperture diameter are approximately equal [13]. In Fig. 5, the non-dimensional description of flow severity is plotted, indicating safe operating conditions with an aperture-normalized swirl number of $0.1 < S_a < 0.25$ and a Reynolds number at the aperture of $1250 < Re_a < 2500$.

c. The influence of cavity flow rate was also found to be significant. Figure 6 shows total tangential flow rates vs. severity level for three levels of total radial and four levels of total cavity flow rates. The most remarkable observation is the difference between zero cavity flow rate and a cavity flow rate of 150 L_n/min. Because the cavity jets are installed at a 45° tangent angle inside the cavity, use of the cavity jets adds significant rotational stability to the cavity region of the reactor, thus augmenting the density of particles available to be pulled into the frustum region of the reactor. As indicated in Fig. 6, the three regions of characteristic flow developed in the frustum region of the reactor were found to be “turbu-

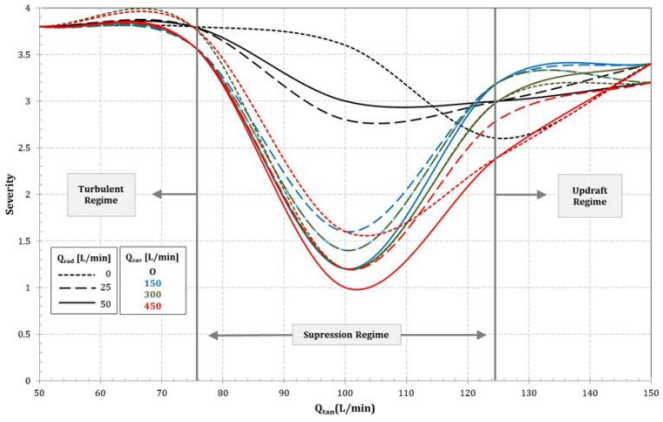

Figure 6: Plot of severity level against tangential flow rate, for a range of radial and cavity flow rates. Characteristic flow regimes are indicated as turbulent, suppression, and updraft. From [9].

lent," "suppression," and "updraft," defined by turbulent breakdown of the fluid flow, stable and fully suppressed particle migration to the frustum, and particle migration via an updraft caused by high levels of rotation, respectively. While it is necessary to operate inside a severity level of 2 in order to avoid particle deposition on the quartz window, this operating range is in fact quite broad. In addition, when operating inside this range and subjecting the reactor to simulated DNI fluctuations, pressure fluctuations on the outlet, and a full reactant feed-cycle, the flow remained fully stable and no window deposition was observed. Of particular note is the steep transition from the optimum operating point where stable flow fully suppresses particle migration, to total flow turbulence with decreasing tangential flow rate (within the space of 10 L_n/min). Although it is beyond the direct scope of this work, temperature gradient related effects can play a significant part in preventing the auxiliary flows of inert gas from protecting the window from particle deposition.

d. The characteristic flow patterns described above are associated with characteristic deposition patterns. Using the visual and IR cameras, a characteristic center-spot deposition pattern was identified to occur when operating in the "updraft" regime for prolonged periods of time. A visual image (A) and IR image (B) can be seen of this center-spot pattern in Fig. 7 (left). In areas where depositions are present on the quartz window, the temperature is increased. When operating in the "turbulent" regime, a ring deposition pattern was observed. A visual (C) and IR (D) image of this pattern can be seen in Fig. 7 (right). Note that angular misalignment of the deposition patterns is due to reactor rotation while the cameras remain fixed. Further, IR temperature data has not been corrected for angular perspective or material characteristics, such as the emittance of the glass.

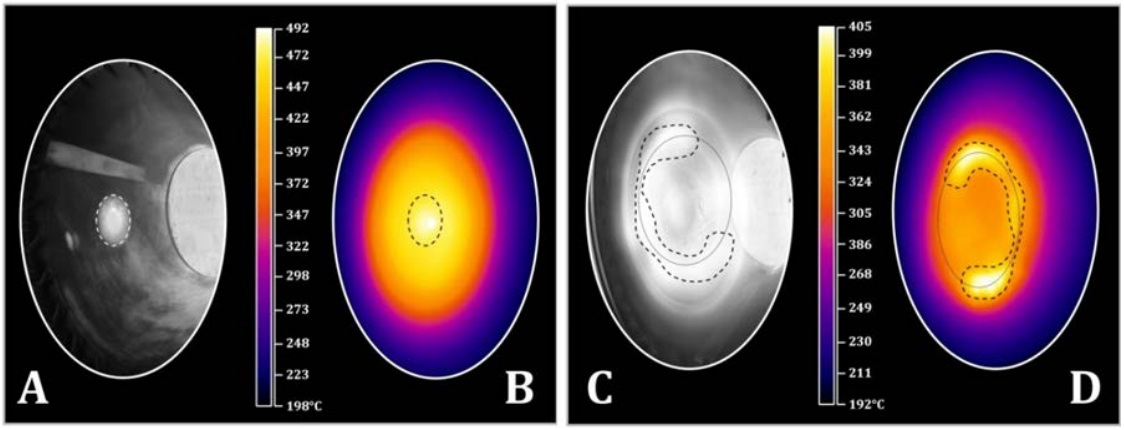

Figure 7: Left: Characteristic center-spot deposition, caused by an updraft, is shown through the visual (A) and IR (B) cameras. Right: Characteristic ring deposition pattern, caused by short exposure to turbulent flow condition, is shown through the visual (C) and IR (D) cameras. From [9].

e. Despite the ability to operate the reactor under conditions where particle deposition on the quartz window is fully suppressed, the capability to clean a fouled window in-situ during an experiment was investigated with the co-injection of CO into the radial jets of the reactor. Figure 8 depicts a sequence of images where, at a fixed Ar radial flow rate of 90 L_n/min, the window begins with characteristic depositions (A) when 1 L_n/min of CO injection is initiated. After 30 min, significant depositions have been removed (B), at which time the CO injection is increased to 5 L_n/min for an additional 10 min. The resulting window (C) has been significantly cleaned, primarily within the hot areas closer to the center of the window. While the center-spot deposition area is fully cleaned, areas lying outside the hottest regions of the window (indicated by the outer dotted white line) retain some of the depositions since the temperature is too low for the carbothermal reduction of ZnO to occur. This region defined by the outer dotted line is, in fact, defined by the region of the window where each light cone from the HFSS lamps intercepts the window.

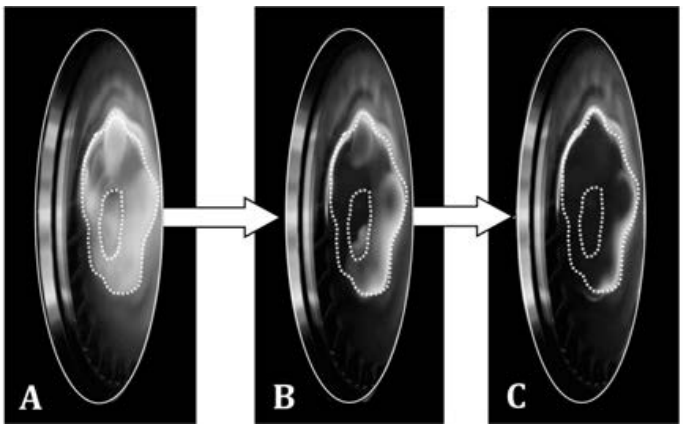

Figure 8: An image sequence of cleaning the quartz window with co-injection of CO.

Publication:

- Koepf E., Villasmil W., Meier A.: ***High temperature flow visualization and aerodynamic window protection of a 100-kWth solar thermochemical receiver-reactor for ZnO dissociation***, Energy Procedia **69**, 1780-1789, 2015. doi: 10.1016/j.egypro.2015.03.148 (**published paper attached**)

  Abstract – A 100-kW_{th} receiver-reactor designed for the thermal dissociation of ZnO into metallic Zn is separated from atmosphere by use of a transparent quartz window, through which concentrated solar radiation is admitted. Protection of such windows from reactant and product particle deposition is critical for successful reactor operation. Using in-situ visualization techniques, the effectiveness of an auxiliary flow of inert gas in aerodynamically protecting a 600-mm-diameter quartz window mounted on the receiver-reactor has been directly assessed during high-temperature experimentation. This work has shown that: (i) high temperature, in-situ flow visualization is possible and effective in assessing flow patterns developed inside the reactor; (ii) there exist three characteristic flow patterns inside the reactor that can be dynamically controlled by use of a set of tangential and radially oriented jets; and (iii) a region of stable protective flow, under a wide range of experimental and operational conditions, is capable of repeatedly and fully suppressing detrimental particle depositions on the quartz window.

WP3:
Solar Pilot Plant Experimental Demonstration at MWSF of PROMES-CNRS in Odeillo

Objectives – Reliable reactor operation without interruption during 8 hours at MWSF. Reproducible experiments with >50% Zn content in the solid product and thermal efficiency exceeding 10%.

Experimental campaign 2014 – The 3rd experimental campaign, initially scheduled for June/July 2014, had to be postponed due to a capacity bottleneck at the solar facility. Eventually, it has been conducted in September/October 2014 at the large-scale solar furnace (MWSF) of *PROMES-CNRS* in Odeillo, France. This solar concentrating research facility, shown in Fig. 9 [15], is comprised of a field of 63 heliostats that track the sun and direct the solar radiation onto a parabolic concentrator, which in turn focuses the sunrays to its focal plane located in the solar tower. For a detailed description of the MWSF and the 2nd experimental campaign with the 100 kW_{th} solar pilot plant see the publication of W. Villasmil et al. [8].

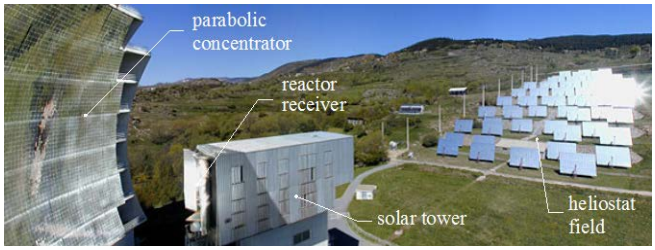

Figure 9: 1 MW solar furnace (MWSF) of *PROMES-CNRS* in Odeillo, France [15].

Description of Work – During the 3rd experimental campaign of 8 weeks, a total of 13 valid on-sun experimental runs, lasting 6-10 hours, have been performed. This low number of experiments is due to the unfavorable weather situation in Odeillo, as can be seen from Fig. 10. Out of 48 possible experimental days, 32 days were cloudy. From the 16 sunny days, 12 days (75%) were used to conduct regular experiments. One experiment (No. 002) had to be stopped prematurely due to increasing cloud coverage. One day (Oct 8, Exp. 010) was lost due to a technical problem, two days were needed for experiment preparations (Sep 13) or repairs (Oct 3), and on one day (Oct 16) no operation was planned.

This work was presented at the SolarPACES2015 Conference and will soon be published in a peer-reviewed journal [16]. A comprehensive summary paper has been accepted (abstract attached at the end of this section). An additional paper dealing with the aerodynamic window protection is being prepared (abstract attached at the end of this section).

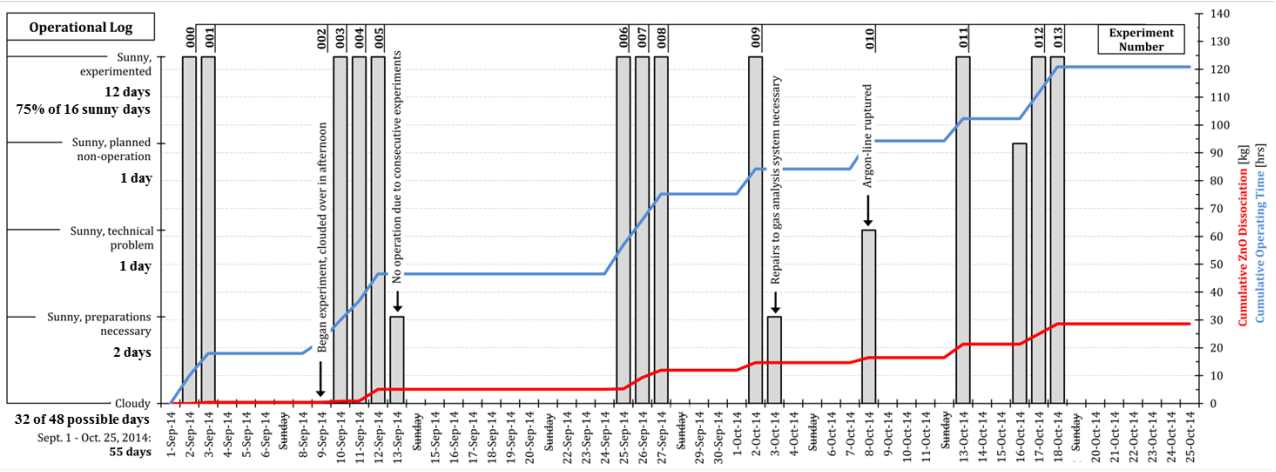

Figure 10: Summary of experiments during the 3rd experimental campaign 2014 in Odeillo, France: The height of the bars indicates the 12 sunny days with experiments conducted, 1 sunny day with planned non-operation, 1 sunny day with a technical problem, 2 days with preparations necessary, and 32 cloudy days out of 48 possible days. The cumulated operating time exceeded 120 hours, and the cumulated ZnO dissociation reached close to 30 kg.

The overview of activities during the 3rd experimental campaign follows the Task structure of this WP.

Task 3.1: Installation and commissioning of 100 kW_{th} pilot plant at the MWSF (25.08.-01.09.2014)

a. The solar pilot plant was shipped by truck from PSI to Odeillo. On August 25, 2014 (the day of arrival), it was mounted on the mobile carriage in focus of the solar tower (Fig. 11). Thanks to the good preparation work at PSI and the experience gained during the previous experimental campaigns, commissioning at the solar tower platform only lasted four days. In parallel, calibration of the heliostats was conducted by PROMES-CNRS.

Figure 11: Solar reactor being moved into the MWSF tower (left) and mounted on experimental platform (right).

b. Functionality tests of all system components included cooling water, gas supply and off-gas piping; electrical connections; electronics; process control and data acquisition systems. Most system components were operating straightaway or after slight modifications.

c. Improved process control and data acquisition systems were used to continuously monitor and control (1) temperatures and pressure inside the solar reactor (Fig. 11, right); (2) cooling water supply for various components such as spillage radiation shield (Fig. 12, left), screw feeder,

Figure 12: Operation of the solar reactor behind the spillage radiation shield on the MWSF tower (left) and visual camera mounted outside the spillage radiation shield on the experimental platform (right).

front shield, front cone, and quench unit; and (3) inert gas supply for aerodynamic window protection and product gas quench. In addition to various webcams surveying the operation of the solar reactor, a visual camera was mounted outside the spillage radiation shield to observe the window and aperture region of the solar reactor from below (Fig. 12, right).

Task 3.2: Experimental campaign at MWSF (02.09.-24.10.2014)

a. Continuous operation and demonstration of the 100-kW_{th} pilot-scale solar thermochemical receiver-reactor was performed at the MWSF, where 13 full-day experiments were conducted utilizing 75% of available sunny days [16]. Figure 13 (left) depicts the solar reactor during operation in the MWSF, and (right) the quartz window acceptably clean after a full-day experiment.

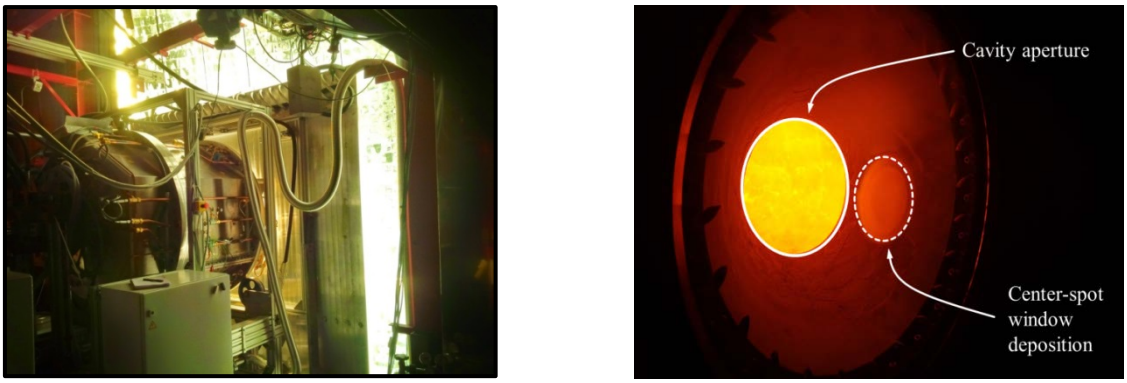

Figure 13: Left: ZnO pilot plant during operation in the MWSF. Right: After an experiment the reaction cavity glows red-hot behind the aperture, and the quartz window is largely free of particulate contamination. From [16].

b. Figure 14 shows a schematic of the solar reactor that was operated at high temperature for over 120 hours, and exposed to input power as high as 125 kW_{th}, with peak radiative fluxes above 4352 suns [16]. Continuous, stable reactor operation was achieved above 2000 K (accumulated time above 30 hours).

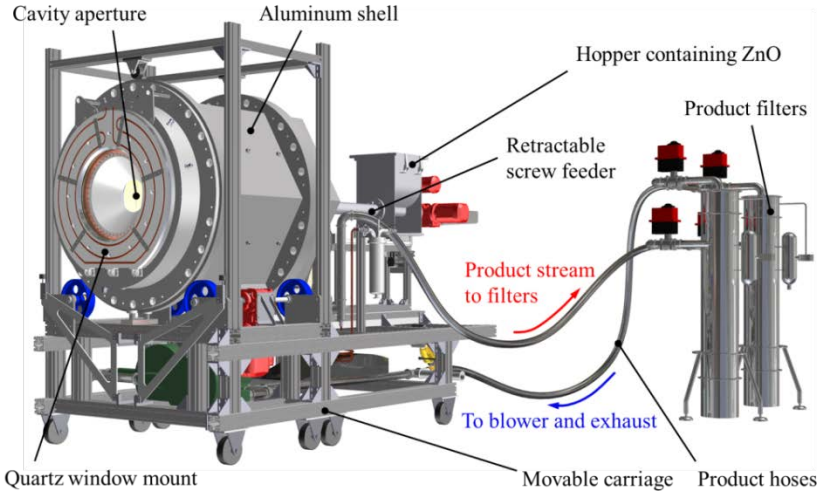

Figure 14: ZnO pilot plant layout utilized in experiments conducted at PSI and Odeillo in 2014, with critical components and peripherals labeled. From [16].

Task 3.3: Performance evaluation

a. ZnO dissociation rates ranged from 1 to 30 g/min and were strongly influenced by cavity temperature, incident radiative flux, and ZnO reactant feed rate. Close to 30 kg of ZnO were dissociated during the demonstration campaign. Figure 15 (left) shows the solar power input Q_{solar}, cavity temperature T, Ar quench flow rate, and O_2 release from the reaction during a repre-

sentative experimental run. The heat-up period was about 4 hours at approximately 6-7 K/min, followed by about 3 hours at peak operating temperatures exceeding 2000 K, measured approx. 15 mm behind the inner surface of the Al_2O_3 bricks forming the cavity wall. Thermal dissociation of ZnO was proven by measuring online O_2 in the product stream. The observed oxygen fluctuation depends on many experimental conditions. Additional chemical species such as N_2, H_2, CO_2, CO, and CH_4 were also monitored to detect and quantify side reactions and/or possible air leakages.

b. Reactor products contained as much as 45% zinc, depending primarily on the amount of quenching argon gas utilized during the experiment.

c. During the experimental campaign, 57 unique experiments were conducted, and performance of the reactor was promising as preliminary results indicate a thermal efficiency as high as 3% at a ZnO dissociation rate of nearly 30 g/min [16]. Figure 15 (right) plots the reactors thermal efficiency and a weighted correlation of solar input power and reactant feed rate against ZnO dissociation rate. The data projects the potential to exceed 10% thermal efficiency at ZnO dissociation rates close to 100 g/min, which is consistent with modeling results. Weather conditions at the MWSF prevented the completion of the experimental plan; ZnO feed rate testing was limited to 1-3.25 kg/hour (10 kg/hour is maximum), resulting in low dissociation rates due to underutilization of the reactors capacity.

d. Peak solar-to-fuel energy conversion efficiency was measured as 0.15 %, and was fundamentally limited by (i) low reactant feed rates due to a shortage of experimental time, and (ii) an ineffective product separation device mounted on the reactor.

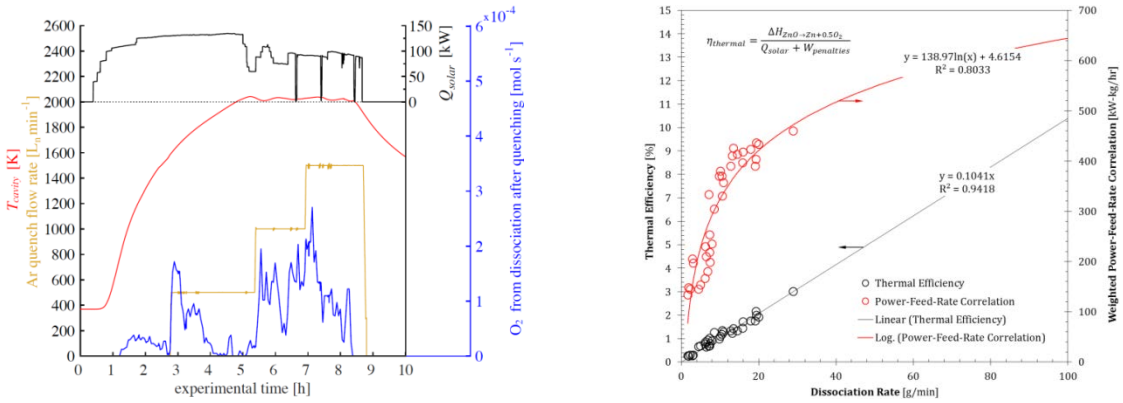

Figure 15: Left: Solar power input Q_{solar}, cavity temperature T_{cavity}, Ar quench flow rate, and O_2 release from dissociation after quenching, measured during a typical experimental run. Right: Reactor thermal efficiency and a weighted correlation of solar input power and reactant feed rate plotted against ZnO dissociation rate. From [16].

Publications:

- E. Koepf, W. Villasmil, A. Meier: ***Demonstration of a 100-kWth High-Temperature Solar Thermochemical Reactor Pilot Plant for ZnO Dissociation***, Proc. 21st SolarPACES Conference, Cape Town, South Africa, October 13-16, 2015; to be published by AIP.
  (**final paper attached, to be *in press* soon**)

  Abstract – Solar thermochemical H2O and CO2 splitting is a viable pathway towards sustainable and large-scale production of synthetic fuels. A reactor pilot plant for the solar-driven thermal dissociation of ZnO into metallic Zn has been successfully developed at the Paul Scherrer Institute (PSI). Promising experimental results from the 100-kWth ZnO pilot plant were obtained in 2014 during two prolonged experimental campaigns in a high flux solar simulator at PSI and a 1-MW solar furnace in Odeillo, France. Between March and June the pilot plant was mounted in the solar simulator and in-situ flow-visualization experiments were conducted in order to prevent particle-laden fluid flows near the window from attenuating transparency by blocking incoming radiation. Window flow patterns were successfully characterized, and it was demonstrated that particle transport could be controlled and suppressed completely. These results enabled the successful operation of the reactor between August and October when on-

sun experiments were conducted in the solar furnace in order to demonstrate the pilot plant technology and characterize its performance. The reactor was operated for over 97 hours at temperatures as high as 2064 K; over 28 kg of ZnO was dissociated at reaction rates as high as 28 g/min.

- E. Koepf, W. Villasmil, A. Meier: ***Pilot-scale Solar Reactor Operation and Characterization for Fuel Production via the Zn/ZnO Thermochemical Cycle***, Appl Energy 2015. (**paper accepted, abstract attached, to be *in press* December 2015**)

  Abstract – Successful demonstration and promising characterization of a solar reactor pilot plant for thermal reduction of ZnO as part of a two-step water and CO_2 splitting cycle has been accomplished at the 100 kW_{th} scale in a 1 MW solar furnace. The solar reactor pilot plant was operated for over 97 hours and achieved sustained reaction temperatures well above 2,000 K, while demonstrating ZnO dissociation rates as high as 28 g/min totaling over 28 kg of processed reactant during 13 full days of experimentation. In-situ high temperature flow visualization of the quartz window enabled the unimpeded operation of the solar reactor, where as many as three consecutive full day experiments were demonstrated without complication. Solar power delivered to the reaction cavity ranged between 90 and 128 kW_{th}, at peak solar concentration ratios as high as 4,671 suns. The products Zn and O_2 were quenched with Ar(g) and recovered in a filter battery, where collected particles contained molar Zn-content as high as 44 %. During experimentation, switching between product collection filter cartridges resulted in 54 unique experiments, where a maximum solar-to-chemical efficiency of 3 % was recorded for the solar reactor. Robust characterization of the product quenching device revealed inherent limitations in its effectiveness, and thus solar-to-fuel energy conversion efficiency was limited to 0.24 % if it would have been possible to supply 4,640 L_n/min of Ar(g). Further, only a limitation on available experimental time prohibited the demonstration of significantly higher dissociation rates, achievable with higher ZnO reactant feed rates. While the use of large volumes of quenching Ar(g) to separate the reaction products remains a significant obstacle to achieving higher solar-to-fuel efficiencies, demonstration of solar reactor technology at the pilot-scale represents significant progress towards the realization of industrial-scale solar fuels production.

- E. Koepf, W. Villasmil, M. Kovacs, A. Meier: ***Demonstration, Optimization, and High Temperature Flow Visualization of Window Protection for a 100-kW Solar Thermochemical Reactor***, J Sol Energy 2016. (**abstract attached**)

  Abstract – Recent successful demonstration of a 100 kW_{th} solar thermochemical reactor pilot plant designed for ZnO dissociation was made possible by the implementation of in-situ, high temperature flow visualization and characterization techniques developed at the Paul Scherrer Institute. Reactant and product ZnO and Zn are contained inside a vortex flow, presenting the possibility of fouling the transparent quartz window through which concentrated sunlight enters and drives the dissociation reaction. Experimental work in a high flux solar simulator delivering 50 kW of radiative power, in addition to characterization and demonstration work in a 1 MW solar furnace delivering 150 kW of radiative power, has shown that: (i) high temperature, in-situ flow visualization is possible and effective in assessing flow patterns developed inside the reactor and actively controlling them; (ii) there exist three characteristic flow patterns inside the reactor that can be dynamically controlled by use of a set of tangential and radially oriented jets; and (iii) a region of stable protective flow, under a wide range of experimental and operational conditions, is capable of repeatedly and fully suppressing detrimental particle depositions on the quartz window. Optimal operating parameters have been determined along with characterization of the condensing particle flows across a wide range of operating conditions.

WP4:
Modeling, Conceptual Design and Economic Assessment

Objectives – Validation of a numerical heat transfer model of the solar reactor for ZnO dissociation; layout and cost estimate of a first-of-its-kind industrial demonstration plant for the production of Zn (e.g. in the power range of 10-50 MW_{th}).

Description of Work – Validation of the solar reactor model has been performed as part of the Ph.D. thesis of W. Villasmil [17] and resulted in a paper on dynamic modeling of the 10 kW_{th} solar reactor prototype tested at *PSI*'s HFSS [18]. A second paper on dynamic modeling of the 100 kW_{th} solar pilot plant at the MWSF is in preparation and will be submitted to a peer-reviewed journal (abstract attached at the end of this section). Evaluation of the work on the conceptual design of a solar industrial plant (Task 4.2) and on system economic analysis (Task 4.3) [19] is in progress and will result in a peer-reviewed journal article (abstract attached at the end of this section).

Task 4.1: Validation of solar reactor model

a. The optical and thermochemical behavior of a 100 kW_{th} solar reactor for the thermal dissociation of ZnO was numerically investigated by applying a detailed simulation model that couples the absorption of the incoming concentrated solar radiation to the heat transfer and chemical reaction occurring within the solar reactor. The geometry of the MWSF was incorporated in a Monte Carlo ray-tracing code to compute the distribution maps of incident solar flux absorbed on the surfaces of the 100 kW_{th} reactor when subjected to the high-flux solar irradiation delivered by the MWSF. After tuning the ray-tracing model vis-à-vis a set of reference heat flux measurements, the ray-tracing code was able to anticipate the solar radiative power input passing through the reactor aperture with an accuracy of 98%. The computed distribution map of incident solar flux absorbed on the reactor surfaces revealed a 59 kW heat loss due to radiation spilled on the water-cooled frustum as a result of the small reactor aperture compared to the MWSF's focal image.

   Coupled to the ray-tracing code, a thermochemical model was used to simulate the processes of chemical reaction and heat transfer occurring within the solar reactor. Experimental validation of the thermochemical model was carried out by comparing predicted temperatures and ZnO dissociation extents with measured data obtained with the 100 kW_{th} solar reactor during on-sun testing at the MWSF in 2012. Among the conducted experiments, the highest experimental efficiency value, $\eta_{solar\ to\ fuel}$ = 0.03%, was obtained at $\overline{T}_{ZnO\ bed}$ = 1853 K and $Q_{solar,\ max}$ = 127 kW. The low efficiency value is a consequence of the large extent of Zn reoxidation (X_{Zn} = 49%) and also presumably the result of mass transport limitations at the ZnO reaction interface, which ultimately leads to slow dissociation kinetics attributed to slow reaction kinetics, presumably as a consequence of mass transport limitations at the ZnO reaction interface. Such limitations translate to the low k_0 value (pre-exponential factor in the Arrhenius kinetic law) found for the 100 kW_{th} reactor ($1.35 \cdot 10^8$ $kg \cdot m^{-3} \cdot s^{-1}$) as compared to the value inferred in a previous study for a 10 kW_{th} reactor prototype, which was 37 times greater. Simulations performed at different values of k_0 corroborated the prominent influence of reaction kinetics on the attainable conversion efficiencies. These simulations indicate the potential of exceeding $\eta_{solar\ to\ fuel}$ = 8% for a k_0 value 10 times the value obtained experimentally in this study. Such an increase may be regarded as conservative considering that the highest reported value k_0 = $2.43 \cdot 10^{10}$ $kg \cdot m^{-3} \cdot s^{-1}$ – determined experimentally using a solar-driven thermogravimeter – is 180 times the value obtained with the 100 kW_{th} reactor.

Task 4.2: Conceptual design of solar industrial plant

a. Prepare layout of industrial demonstration plant for solar Zn production (e.g. 10-50 MW_{th}) by sizing of components and calculation of material and energy flows.

Task 4.3: System economic analysis

a. Model and predict system economics of solar Zn production plant.

b. Estimate cost of solar industrial plant.

Work on the conceptual design of a solar industrial plant (Task 4.2) and on system economic analysis (Task 4.3) has been performed in the framework of a master thesis [19].

Publications:

- W. Villasmil, T. Copper, E. Koepf, A. Meier, A. Steinfeld: ***Coupled Ray-Tracing, Heat Transfer, and Thermochemical Modeling of a 100-kW$_{th}$ High Temperature Solar Reactor for Thermal Dissociation of ZnO***, Energy&Fuels 2016. (**abstract attached**)

  Abstract – This work reports a numerical investigation of the unsteady-state operation of a 100-kW$_{th}$ solar reactor for performing the high-temperature step of the Zn/ZnO thermochemical cycle for syngas production. The solar two-step Zn/ZnO redox cycle comprises: (1) the endothermal dissociation of ZnO to Zn and O_2 above 2000 K using concentrated solar energy, and (2) the subsequent exothermal oxidation of Zn with H_2O/CO_2 to produce H_2/CO and recover the initial ZnO. The performance of the 100-kW$_{th}$ solar reactor is investigated using a dynamic numerical model consisting of two coupled sub-models. The first is a Monte Carlo ray-tracing model applied to compute the distribution maps of incident solar flux absorbed on the reactor surfaces when subjected to high-flux solar irradiation delivered by the PROMES-CNRS MegaWatt Solar Furnace (MWSF). The second is a heat transfer, thermochemical model that uses the computed maps of absorbed solar flux as radiation boundary condition to simulate the coupled processes of chemical reaction and heat transfer by radiation, convection, and conduction. After parameter tuning of the mirror optical properties, the ray-tracing code is able to anticipate the reactor's solar radiative power input with an accuracy of 98%. Experimental validation of the reactor model is accomplished by comparing predicted temperatures and ZnO dissociation extents with measured data acquired with the 100-kW$_{th}$ solar reactor at the MWSF. The experimentally obtained solar-to- chemical energy conversion efficiencies are reported and the various energy flows are quantified. The model shows the prominent influence of reaction kinetics on the attainable conversion efficiencies, revealing the potential of achieving $\eta_{solar\text{-}to\text{-}chemical}$ = 16% if the mass transport limitations on the ZnO reaction interface were overcome.

- E. Koepf, W. Villasmil, R. Jakober, A. Meier: ***Techno-Economic Analysis of an Industrial Plant for Hydrogen Production via the Zn/ZnO Solar Thermochemical Cycle***, J Energy 2016. (**abstract attached**)

  The production of hydrogen and/or syngas via solar water and CO_2 splitting thermochemical cycles offers an attractive pathway towards large scale and renewable solar fuel production. An in-depth techno-economic analysis of industrial-scale hydrogen production via the Zn/ZnO solar-thermochemical cycle has been performed, incorporating state-of-the-art solar reactor development, and realistic technical and energetic assumptions, including quasi-steady state reactor operation resulting in dynamic reactor temperatures, and the energy required to separate high temperature reaction products Zn and O2. A 110-MW$_{th}$ solar-hydrogen production plant located in Daggett, CA served as a base-case for the analysis, and a hydrogen production price of 8.36 $/kg was determined when practical design considerations are incorporated and no heat-recovery nor product separation energy penalty is assumed. Results indicate a very strong cost-dependence on the price of the heliostat field, as expected, comprising as much as 70% of the direct cost when the installed heliostat price is 151 $/m^2. The impact of inert gas consumption on the process economics is significant; by considering realistic product separation technology and a conservative cost of recycling inert gas from the product stream, a hydrogen price of 31.21 $/kg is determined. This analysis indicates that the far-term price of hydrogen by the Zn/ZnO solar thermochemical cycle becomes 6.20 $/kg with significant technical advances, which approaches the US Department of Energy near-term hydrogen production target of 6 $/kg, but is still far from its far-term goal of 3 $/kg. Thus, significant advances in the technology related to the Zn/ZnO thermochemical cycle are required to make it an economically competitive pathway towards solar fuel production.

National Cooperation

The Solar Technology Laboratory at *PSI* is working jointly with the Professorship in Renewable Energy Carriers at *ETH* Zürich.

National cooperation is performed within the framework of

- *Hydropole – Swiss Hydrogen Association* (*PSI* Representative: Dr. Christian Wieckert)
- *Solar Receiver Development for Concentrating Solar Power Systems* (Industrial Project with *ALE AirLight*) – Solar receiver coupled with trough concentrator for a Rankine-based electricity generation system.
- *High-temperature Thermal Storage System for Concentrating Solar Power* (Industrial Project with *ALE AirLight*) – Cost-effective and efficient thermal storage based on a packed bed of rocks with air as working fluid.
- *Inflated Photovoltaic Ultra-light Mirror Concentrators* (Industrial Project with *ALE AirLight*) – Cost-competitive innovative concentrating photovoltaic (CPV) system
- *Solar-driven Combined Cycles* (Industrial Project with *Alstom*) – Novel solar receiver for heating compressed air to the entrance conditions of a gas turbine, as part of a combined cycle for power generation.
- *Solar Fuels for Cement Manufacturing* (Industrial Project with *Holcim*) – High-temperature solar heat for upgrading carbonaceous feedstock to produce high-quality syngas.
- *CCEM HyTech* – Sustainable hydrogen technologies (*EPFL, Empa*)
- *CCEM SolarHTG* – Solar assisted hydrothermal gasification process (*EPFL, ALE Airlight*)

Current collaboration with Swiss companies:

Switzerland	*ALE Airlight Energy SA,* Biasca
	Alstom Power Service, Baden-Dättwil; *Alstom Power Systems,* Birr
	Bühler AG, Uzwil
	Climeworks Ltd., Zürich
	Holcim, Holderbank
	IBM, Rüschlikon

Current collaboration and synergism with other Swiss research laboratories:

Switzerland	*EMPA* Dübendorf – Laboratory for Solid State Chemistry and Catalysis (Prof. A. Weidenkaff)
	EMPA Dübendorf – Laboratory for Hydrogen and Energy (Dr. U. Vogt)
	EPFL Lausanne – Laboratory of Renewable Energy Science and Engineering (Prof. S. Haussener)
	EPFL Lausanne – Industrial Energy System Laboratory (Prof. F. Maréchal)
	ETH Zürich – Particle Technology Laboratory (Prof. S. Pratsinis)
	SUPSI Manno – Department of Innovative Technologies (Prof. M. Barbato)
	University of Zurich – Institute of Inorganic Chemistry (G. Patzke)

International Cooperation

International cooperation is being performed within the framework of

- *EERA – European Energy Research Alliance*. ***Joint Program on Concentrated Solar Power (CSP)****.* Swiss Representative at EERA ExCo: Urs Elber, Managing Director CCEM, PSI; Swiss Representative for CSP Joint Program and Coordinator of Sub-Program Solar Fuels: Dr. A. Meier.
- *IEA's SolarPACES Implementing Agreement* (Task II – ***Solar Chemistry Research***; Operating Agent: Dr. A. Meier)
- *IPHE – International Partnership for the Hydrogen Economy* (Project: ***Solar driven high temperature thermochemical production of hydrogen***; Swiss Representative: Prof. Dr. A. Steinfeld). Participants: *CIEMAT* (Spain), *CNRS* (France), *DLR* (Germany), *U. Colorado* (USA), *ETH* & *PSI* (Switzerland), *NU* & *TIT* (Japan), *WIS* (Israel).
- *SFERA II – Solar Facilities for the European Research Area* (EU Project). Partners: *CIEMAT* (Spain), *CNRS* (France), *DLR* (Germany), *ETHZ* & *PSI* (Switzerland), *ENEA* (Italy), *CEA-INES* (France), *INESC-ID* (Portugal), *UEVORA* (Portugal), *UNILIM* (France), *ESTELA* (Belgium), *UTV* (Italy); PSI Project Manager: Dr. Christian Wieckert
- *SOLLAB – Alliance of European Laboratories on solar thermal concentrating systems*. Collaboration of leading European solar research laboratories, namely *CIEMAT* (Spain), *CNRS* (France), *DLR* (Germany), *ETH* & *PSI* (Switzerland); Swiss Representative: Prof. A. Steinfeld.
- *STAGE-STE – Scientific and Technological Alliance for Guaranteeing the European Excellence in Concentrating Solar Thermal Energy* (EU Project, start February 2014). Partners: 22 European research organizations, 8 European industrial companies, 10 international research organizations. Coordinator of Work Package on Solar Thermochemical Fuels: Dr. Anton Meier
- *TCSPower – Thermo-chemical energy storage for concentrated solar power plants* (EU Project). Partners: DLR (Germany), Siemens Concentrated Solar Power LTD (Israel), Bühler AG (Switzerland), Eramet & Comilog Chemicals SA (Belgium), IMDEA *Energías* (Spain), PSI (Switzerland), Universität Siegen (Germany); PSI Project Manager: Dr. Christian Wieckert
- *Strategic Alliance* between *PSI* and *CIEMAT* (Spain) – Roadmap to Solar H_2 Production.

Current collaboration and synergism with other international research laboratories:

Australia	*ANU* – Australian National University, Canberra *CSIRO* – Commonwealth Scientific and Industrial Research Organisation, Newcastle, NSW
Austria	*Energy Research Center, Vorarlberg University of Applied Sciences, Dornbirn*
France	*PROMES-CNRS* – Centre National de la Recherche Scientifique, Odeillo
Germany	*DLR* – Deutsches Zentrum für Luft- und Raumfahrt, Köln & Stuttgart
Israel	*WIS* – Weizmann Institute of Science, Rehovot
Italy	*ENEA* – Italian National Agency for New Technologies, Energy and Sustainable Economic Development, Roma
Japan	*TIT* – Tokyo Institute of Technology, Tokyo *NU* – Niigata University, Niigata
Spain	*CIEMAT* – Centro de Investigaciones Energéticas, Medioambientales y Tecnológicas, Madrid & Almería *IMDEA* Energías – Instituto Madrileño de Estudios Avanzados, Móstoles
USA	*Caltech* – California Institute of Technology, Pasadena, USA *NREL* – National Renewable Energy Laboratories, Golden, CO *SNL* – Sandia National Laboratory, Albuquerque, NM, & Livermore, CA *UC* – University of Colorado, Boulder, CO *UD* – University of Delaware, Newark, DE *UF* – University of Florida, Gainesville, FL *UM* – University of Minnesota, Minneapolis, MN

Evaluation

Achievements

The following papers result from this project:

1. Villasmil W, Brkic M, Wuillemin D, Meier A, Steinfeld A. Pilot Scale Demonstration of a 100-kW_{th} Solar Thermochemical Plant for the Thermal Dissociation of ZnO. J Sol Energy Eng 2013;136:011017. doi:10.1115/1.4025512. (**published paper attached**)
2. Koepf E, Villasmil W, Meier A. High Temperature Flow Visualization and Aerodynamic Window Protection of a 100-kWth Solar Thermochemical Receiver-reactor for ZnO Dissociation. Energy Procedia 2015;69:1780–9. doi:10.1016/j.egypro.2015.03.148. (**published paper attached**)
3. Koepf E, Villasmil W, Meier A. Demonstration of a 100-kWth High-Temperature Solar Thermochemical Reactor Pilot Plant for ZnO Dissociation, presented at Solar PACES 2015, to be published by AIP. (**final paper attached, to be *in press* soon**)
4. Koepf E, Villasmil W, Meier A. Pilot-scale Solar Reactor Operation and Characterization for Fuel Production via the Zn/ZnO Thermochemical Cycle. Appl Energy 2015. (**paper accepted, abstract attached, to be *in press* December 2015**)
5. Koepf E, Villasmil W, Kovacs M, Meier A. Demonstration, Optimization, and High Temperature Flow Visualization of Window Protection for a 100-kW Solar Thermochemical Reactor. J Sol Energy 2016. (**abstract attached**)
6. Villasmil W, Copper T, Koepf E, Meier A, Steinfeld A. Coupled Ray-Tracing, Heat Transfer, and Thermochemical Modeling of a 100-kWth High Temperature Solar Reactor for Thermal Dissociation of ZnO. Energy&Fuels 2016. (**abstract attached**)
7. Koepf E, Villasmil W, Jakober R, Meier A. Techno-Economic Analysis of an Industrial Plant for Hydrogen Production via the Zn/ZnO Solar Thermochemical Cycle. J Energy 2016. (**abstract attached**)

Outlook

In conclusion of this project, a detailed technical assessment has been performed. The purpose of performing detailed technical assessments on specific components of the 100 kW_{th} solar reactor developed inside the Solar Technology Laboratory (STL) at the Paul Scherrer Institute (PSI) was to ensure a complete and adequate closure of the technology development and demonstration project. With more than 10 years of experience bringing this reactor concept to fruition and successful demonstration at the 100 kW_{th} scale, the STL has an obligation of knowledge and technology transfer to the scientific community. Beyond the scope of publications in peer reviewed journals and conference presentations, this technical assessment covers specific details that can be of value to scientists and engineers interested in pursuing a related line of research and development, or even developing the same solar reactor technology directly.

(**An index of the technical assessment is attached to this report**)

Publications

The following is a list of recent publications of the Solar Technology Laboratory at PSI and the Professorship of Renewable Energy Carriers at ETH Zurich, originating from or related to the *Solar Zinc Project* [1].

Books and Book Chapters

- Robinson A., Steinfeld A.: ***Brewing fuels in a solar furnace***, In: *MRS Bulletin – Energy Quarterly*, Vol. 38, 208-209, 2013.
- Meier A.: ***Life cycle analysis and economic assessment of solar hydrogen***, In: *Handbook of Hydrogen Energy*. Edited by S.A. Sherif, D.Y. Goswami, E.K. Stefanakos, and A. Steinfeld, CRC Press 2014, Print ISBN: 978-1-4200-5447-7, eBook ISBN: 978-1-4200-5450-7, Chapter 14, pp. 537-563, 2014.
- Sherif S.A., Goswami D.Y., Stefanakos E.K., Steinfeld A.: ***Handbook of Hydrogen Energy***, CRC Press, ISBN 978-1-4200-5447-7, 2014.
- Weidenkaff A., Trottmann M., Tomeš P., Suter C., Steinfeld A., Veziridis A.: ***Solar TE Converter Applications***, In: *Thermoelectric Nanomaterials,* Springer Series in Materials Science, Vol. 182, Chapter 16, 365-382, 2013.

Peer-reviewed Journals

- Ackermann S., Scheffe J.R., Steinfeld A.: ***Diffusion of Oxygen in Ceria at Elevated Temperatures and its Application to H2O/CO2-Splitting Thermochemical Redox Cycles***, J. Physical Chemistry **118**, 5216-5225, 2014. doi:10.1021/jp500755t
- Ackermann S., Scheffe J.R., Duss J., Steinfeld A.: ***Morphological Characterization and Effective Thermal Conductivity of Dual-Scale Reticulated Porous Structures***, Materials **7**, 7173-7195, 2014. doi:10.3390/ma7117173
- Alonso E., Hutter C., Romero M., Steinfeld A., Gonzalez-Aguilar J.: ***Kinetics of Mn2O3-to-Mn3O4 and Mn3O4-to-MnO redox reactions performed under concentrated thermal radiative flux***, Energy & Fuels **27**, 4884-4890, 2013. DOI:10.1021/ef400892j
- Alxneit I., Tschudi R.: ***Modeling the Formation and Chemical Composition of Partially Oxidized Zn/ZnO Particles Formed by Rapid Cooling of a Mixture of Zn(g) and O2***, Journal of Materials **2013**, 718525, 2013. DOI:10.1155/2013/718525
- Bader R., Pedretti P., Barbato M., Steinfeld A.: **An Air-Based Corrugated Cavity-Receiver for Solar Parabolic Trough Concentrators**, Applied Energy **138**, 337-345, 2015. DOI:10.1016/j.apenergy.2014.10.050
- Cooper T., Ambrosetti G., Pedretti A., Steinfeld A.: ***Theory and design of line-to-point focus solar concentrators with tracking secondary optics***, Applied Optics **52**, 8586-8616, 2013. DOI:10.1364/AO.52.008586
- Cooper T., Dähler F., Ambrosetti G., Pedretti A., Steinfeld A.: ***Performance of compound parabolic concentrators with polygonal apertures***, Solar Energy **95**, 308-318, 2013. DOI:10.1016/j.solener.2013.06.023
- Cooper T., Pravettoni M., Cadruvi M., Ambrosetti G., Steinfeld A.: ***The effect of irradiance mismatch on a semi-dense array of triple-junction concentrator cells***, Solar Energy Materials and Solar Cells **116**, 238-251, 2013. DOI:10.1016/j.solmat.2013.04.027
- Cooper T., Schmitz M., Good P., Ambrosetti G., Pedretti A., Steinfeld A.: ***Non-parabolic solar concentrators matching the parabola***, Optical Letters **39**, 4301-4304, 2014. doi:10.1364/OL.39.004301
- Durgasri D., Viodkumar T., Lin F., Alxneit I., Reddy B.: ***Gadolinium doped cerium oxide for soot oxidation: Influence of interfacial metal–support interactions***, Applied Surface Science **314**, 592–598, 2014. doi:10.1016/j.apsusc.2014.07.036
- Ezbiri M., Allen K., Gàlvez M., Michalsky R., Steinfeld A.: ***Design Principles of Perovskites for Thermochemical Oxygen Separation***, ChemSusChem **8**, 1966-1971, 2015. DOI:10.1002/cssc.201500239

- Fernández-García A., Cantos-Soto M.E., Röger M., Wieckert C., Hutter C., Martínez-Arcos L.: ***Durability of solar reflector materials for secondary concentrators used in CSP systems***, Solar Energy Materials and Solar Cells **130**, 51-63, 2014. doi:10.1016/j.solmat.2014.06.043
- Friess H., Haussener S., Steinfeld A., Petrasch J.: ***Tetrahedral mesh generation based on space indicator functions***, International Journal for Numerical Methods in Engineering **93**, 1040-1056, 2013. DOI:10.1002/nme.4419
- Furler P., Scheffe J., Marxer D., Gorbar M., Bonk A., Vogt U., Steinfeld A.: ***Thermochemical CO2 Splitting via Redox Cycling of Ceria Reticulated Foam Structures with Dual-Scale Porosities***, Physical Chemistry Chemical Physics **16**, 10503-10511, 2014. doi:10.1039/c4cp01172d
- Gebald C., Wurzbacher J.A., Tingaut P., Steinfeld A.: ***Stability of Amine-Based Cellulose during Temperature-Vacuum Swing Cycling for CO2 Capture from Air***, Environmental Science & Technology **47**, 10063-10070, 2013. DOI:10.1021/es401731p
- Gebald C., Wurzbacher J., Borgschulte A., Zimmermann T., Steinfeld A.: ***Single-Component and Binary CO_2 and H_2O Adsorption of Amine-Functionalized Cellulose***, Environmental Science & Technology **48**, 2497-2504, 2014. DOI:10.1021/es404430g
- Good P., Ambrosetti G., Pedretti A., Steinfeld A.: ***An array of coiled absorber tubes for solar trough concentrators operating with air at 600°C and above*****,** Solar Energy **111**, 378-395, 2015. DOI:10.1016/j.solener.2014.09.016
- Halmann M., Steinfeld A., Epstein M., Vishnevetsky I.: ***Vacuum Carbothermic Reduction of Alumina***, Mineral Processing and Extractive Metallurgy Review **35**, 126 – 135, 2014. DOI:10.1080/08827508.2012.706762
- Halmann M., Steinfeld A.: ***Reforming of Blast Furnace Gas with Methane, Steam, and Lime for Syngas Production and CO2 Capture: A Thermodynamic Study***, Mineral Processing and Extractive Metallurgy Review **36**, 7-12, 2015. doi:10.1080/08827508.2013.793682
- Koepf E., Advani S.G., Prasad A.K., Steinfeld A.: ***Experimental Investigation of the Carbothermal Reduction of ZnO Using a Beam-Down, Gravity-Fed Solar Reactor***, Industrial & Engineering Chemistry Research **54**, 8319-8332, 2015. DOI:10.1021/acs.iecr.5b01249
- Koepf E., Villasmil W., Meier A.: ***High temperature flow visualization and aerodynamic window protection of a 100-kWth solar thermochemical receiver-reactor for ZnO dissociation***, Energy Procedia **69**, 1780-1789, 2015. DOI:10.1016/j.egypro.2015.03.148
- Kruesi M., Jovanovic Z.R., dos Santos E., Yoon H.C., Steinfeld A.: ***Solar-driven steam-based gasification of sugarcane bagasse in a combined drop-tube and fixed-bed reactor – Thermodynamic, kinetic, and experimental analyses***, Biomass and Bioenergy **52**, 173-183, 2013. DOI:10.1016/j.biombioe.2013.03.003
- Kruesi M., Jovanovic Z.R., Steinfeld A.: ***A Two-Zone Solar-Driven Gasifier Concept: Reactor Design and Experimental Evaluation with Bagasse Particles***, Fuel **117**, 680 – 687, 2014. DOI:10.1016/j.fuel.2013.09.011
- Kruesi M., Jovanovic Z.R., Haselbacher A., Steinfeld A.: ***Analysis of Solar-Driven Gasification of Biochar Trickling through an Interconnected Porous Structure***, AIChE Journal **61**, 367-879, 2015. DOI:10.1002/aic.14672
- Lichty P., Wirz M., Kreider P., Kilbury O., Dinair D., King D., Steinfeld A., Weimer W.A.: ***Surface Modification of Graphite Particles Coated by Atomic Layer Deposition and Advances in Ceramic Composites***, International Journal of Applied Ceramic Technology **10**, 257-265, 2013. DOI:10.1111/j.1744-7402.2012.02750.x
- Lin F., Alxneit I., Wokaun A.: **Rh-doped ceria: solar organics from H2O, CO2 and sunlight**, Energy Procedia **69**, 1790-1799, 2015. DOI:10.1016/j.egypro.2015.03.151
- Lin F., Alxneit I., Wokaun A.: ***Structural and chemical changes of Zn-doped CeO2 nanocrystals upon annealing at ultra-high temperatures***, CrystEngComm **17**, 1646-1653, 2015. DOI:10.1039/c4ce02202e
- Lin F., Delmelle R., Vinodkumar T., Reddy B.M., Wokaun A., Alxneit I.: ***Correlation between the structural characteristics, oxygen storage capacities and catalytic activities of dual-phase Zn-modified ceria nanocrystals***, Catalysis Science & Technology **5**, 3556-3567, 2015. DOI:10.1039/c5cy00351b

- Lipinski W., Davidson J.H., Haussener S., Klausner J.F., Mehdizadeh A.M., Petrasch J., Steinfeld A.: ***Review of heat transfer research for solar thermochemical applications***, Journal of Thermal Science and Engineering Applications **5**, 021005-1/14, 2013. DOI:10.1115/1.4024088
- Marti J., Roesle M., Steinfeld A.: ***Experimental determination of the radiative properties of particle suspensions for high-temperature solar receiver applications***, Heat Transfer Engineering **35**, 272-280, 2013. DOI:10.1080/01457632.2013.825173
- Marti J., Roesle M., Steinfeld A.: ***Combined Experimental-Numerical Approach to Determine Radiation Properties of Particle Suspensions***, J. Heat Transfer **136**, 092701-1/7, 2014. doi:10.1115/1.4027768
- Pozivil P., Ettlin N., Stucker F., Steinfeld A.: ***Modular Design and Experimental Testing of a 50 kWth Pressurized-Air Solar Receiver for Gas Turbines*****,** J. Solar Energy Eng. **137**, 031002-1/7, 2015. DOI:10.1115/1.4028918
- Roeb M., Haussener S., Steinfeld A.: ***Sulphur based thermochemical cycles: Development and assessment of key components of the process***, International Journal of Hydrogen Energy **38**, 6197-6204, 2013. DOI:10.1016/j.ijhydene.2013.01.068
- Scheffe J., Jacot R., Patzke G., Steinfeld A.: ***Synthesis, Characterization and Thermochemical Redox Performance of Hf, Zr and Sc Doped Ceria for Splitting CO2***, Journal of Physical Chemistry B **177**, 24104-24114, 2013. DOI:10.1021/jp4050572
- Scheffe J.R., Weibel D., Steinfeld A.: ***Lanthanum-strontium-manganese perovskites as redox materials for solar thermochemical splitting of H2O and CO2***, Energy & Fuels **27**, 4250–4257, 2013. DOI:10.1021/ef301923h
- Scheffe J.R., Welte M., Steinfeld A.: ***Thermal reduction of ceria within an aerosol reactor for H2O and CO2 splitting***, Ind. & Eng. Chem. Res. **56**, 2175-2182, 2014. doi:10.1021/ie402620k
- Scheffe J.R., Steinfeld A.: ***Oxygen Exchange Materials for Solar Thermochemical Splitting of H2O and CO2 – A Review***, Materials Today **17**, 341-348, 2014. doi:10.1016/j.mattod.2014.04.025
- Sehaqui H., Gálvez M.E., Becattini V., Ng Y., Steinfeld A., Zimmermann T., Tingaut P.: ***Fast and reversible direct CO2 capture from air onto all-polymer Nanofibrillated cellulose – Polyethyleneimine foams***, Environmental Science & Technology **49**, 3167-3174, 2015. DOI:10.1021/es504396v
- Stamatiou A., Steinfeld A., Jovanovic Z.R.: ***On the effect of the presence of solid diluents during Zn oxidation by CO2***, Industrial & Engineering Chemistry Research **52**, 1859-1869, 2013. DOI:10.1021/ie302643g
- Steinfeld A.: ***Materials and Processes for Renewable Energy Technologies***, Journal of Metals **65**, 1658-1659, 2013. DOI:10.1007/s11837-013-0792-z
- Stroehle S., Haselbacher A., Jovanovic Z., Steinfeld A.: ***Transient Discrete-Granule Packed-Bed Reactor Model for Thermochemical Energy Storage***, Chem. Eng. Sci. **117**, 465-478, 2014. doi:10.1016/j.ces.2014.07.009
- Suter S., Steinfeld A., Haussener S.: **Pore-level engineering of macroporous media for increased performance of solar-driven thermochemical fuel processing**, Int. J. Heat and Mass Transfer **78**, 688-698, 2014. doi:10.1016/j.ijheatmasstransfer.2014.07.020
- Tzouganatos N., Matter R., Wieckert C., Antrekowitsch J., Gamroth M., Steinfeld A.: ***Thermal Recycling of Waelz Oxide using Concentrated Solar Energy***, Journal of Metals **65**, 1733-1743, 2013. DOI:10.1007/s11837-013-0778-x
- Tzouganatos N., Dell'Amico M., Wieckert C., Hinkley J., Steinfeld A.: ***On the Development of a Zinc Vapor Condensation Process for the Solar Carbothermal Reduction of Zinc Oxide***, Journal of Metals **67**, 1096-1109, 2015. DOI:10.1007/s11837-015-1356-1
- Venkataswamy P., Jampaiah D., Lin F., Alxneit I., Reddy B.M.: ***Structural properties of alumina supported Ce-Mn solid solutions and their markedly enhanced catalytic activity for CO oxidation***, Applied Surface Science **349**, 299–309, 2015. DOI:10.1016/j.apsusc.2015.04.220
- Villasmil W., Brkic M., Wuillemin D., Meier A., Steinfeld A.: ***Pilot scale demonstration of a 100-kWth solar thermochemical plant for the thermal dissociation of ZnO***, ASME Journal of Solar Energy Engineering **136**, 011017-1/11, 2014. DOI:10.1115/1.4025512

- Villasmil W., Meier A., Steinfeld A.: ***Dynamic modeling of a solar reactor for zinc oxide thermal dissociation and experimental validation using IR thermography***, ASME Journal of Solar Energy Engineering **136**, 011015-1/11, 2014. DOI:10.1115/1.4025511
- Viodkumar T., Durgasri D., Reddy B., Alxneit I.: ***Synthesis and structural characterization of Eu2O3 doped CeO2: Influence of oxygen defects on CO oxidation***, Catalysis Letters **144** (12), 2033-2042, 2014. doi:10.1007/s10562-014-1367-5
- Wieckert C., Obrist A., von Zedtwitz P., Maag G., Steinfeld A.: ***Syngas production by thermochemical gasification of carbonaceous waste materials in a 150 kWth packed-bed solar reactor***, Energy & Fuels **27**, 4884-4890, 2013. DOI:10.1021/ef4008399
- Wirz M., Petit J., Haselbacher A., Steinfeld A.: ***Potential Improvements in the Optical and Thermal Efficiencies of Parabolic Trough Concentrators***, Solar Energy **107**, 398-414, 2014. doi:10.1016/j.solener.2014.05.002
- Wirz M., Roesle M., Steinfeld A.: ***Design point for predicting year-round performance of solar parabolic trough concentrator systems***, ASME Journal of Solar Energy Engineering **136**, 021019-1/7, 2014. doi:10.1115/1.4025709
- Zanganeh G., Commerford M., Haselbacher A., Pedretti A., Steinfeld A.: ***Stabilization of the Outflow Temperature of a Packed-Bed Thermal Energy Storage by Combining Rocks with Phase Change Materials***, Applied Thermal Engineering **70**, 316-320, 2014. doi: 10.1016/j.applthermaleng.2014.05.020
- Zanganeh G., Pedretti A., Haselbacher A., Steinfeld A.: ***Design of Packed-Bed Thermal Energy Storage Systems for High-Temperature Industrial Process Heat***, Applied Energy **137**, 812-822, 2015. DOI:10.1016/j.apenergy.2014.07.110
- Zermatten E., Schneebeli M., Arakawa H., Steinfeld A.: ***Tomography-based determination of porosity, specific area and permeability of snow and comparison with measurements***, Cold Regions Science and Technology **97**, 33-40, 2014. DOI:10.1016/j.coldregions.2013.09.013
- Zermatten E., Vetsch J.R., Ruffoni D., Hofmann S., Müller R., Steinfeld A.: ***Micro-computed tomography based computational fluid dynamics for the determination of shear stresses in scaffolds within a perfusion bioreactor***, Annals of Biomedical Engineering **42**, 1085-1094, 2014. doi:10.1007/s10439-014-0981-0

Dissertation

- Villasmil W.: ***Dynamic Modeling and Experimental Demonstration of a 100-kW$_{th}$ Solar Thermochemical Reactor for ZnO Dissociation***, PhD Thesis Nr. 21675, ETH Zürich, December 2013.

Master Theses

- Gasser M.: ***Development and testing of a measurement method to estimate the particle cloud density of ZnO particles***, PSI Villigen and ETH Zürich, December 2013.
- Geissbühler L.: ***Experimental investigation of chemical kinetics for thermochemical storage***, PSI Villigen and ETH Zürich, October 2013.
- Jakober R.: ***Conceptual design of an industrial solar thermochemical plant for ZnO dissociation***, PSI Villigen and ETH Zürich, February 2015.

Conference Proceedings / Other Papers

- Bader R., Gampp L., Steinfeld A., Lipinski W.: ***Transient radiative heat transfer in a suspension of ceria particles undergoing non-stoichiometric reduction***, Proc. 11th AIAA/ASME Joint Thermophysics and Heat Transfer Conference, Atlanta, USA, June 16-20, 2014.
- Bader R., Steinfeld A.: ***Solar Trough Concentrator Design for Uniform Radiative Flux Distribution***, Optical Society of America Light, Energy and the Environment Congress, Canberra, Australia, December 2-5, 2014.
- Balomnenos E., Diamantopoulos P., Gerogiorgis D., Panias D., Paspaliaris I., Kemper C., Friedrich B., Vishnevetsky I., Epstein M., Halmann M., Haselbacher A., Jovanovic Z., Steinfeld A.: ***Investigations into innovative and sustainable processes for the carbothermic produc-***

tion of gaseous aluminum, TMS Conference Proceedings: Light Metals 2014: Aluminum Reduction Technology, San Diego, USA, February 16-20, 2014.

- Bhosale R.R., Alxneit I., van den Broeke L.L.P., Kumar A., Jilani M., Gharbia S.S., Folady J., Dardor D. Z.: ***Sol-gel synthesis of nanocrystalline Ni-ferrite and Co-ferrite redox materials for thermochemical production of solar fuels,*** 2014 MRS Spring Meeting, San Francisco, CA, USA, April 21-25, 2014; doi:10.1557/opl.2014.866, Mater. Res. Soc. Symp. Proc. **1675,** 203-208, 2014.
- Clavin M., Steinfeld A.: ***Estudio preliminar de la posibilidad de utilización de energía solar térmica concentrada en Argentina***, Acta de la XXXVI Reunión de trabajo de la Asociación Argentina de Energías Renovables y Medio Ambiente. Vol. 1, pp. 09.09-09.18, ISBN 978-987-29873-0-5, San Miguel de Tucumán, Argentina, October 22-25, 2013.
- Furler P., Scheffe J.R., Gorbar M., Moes L., Vogt U., Steinfeld A.: ***Solar thermochemical CO2 splitting utilizing a reticulated porous ceria redox system***, Proc. ACS Annual Meeting, New Orleans, USA, April 7-11, 2013.
- Goel N., Gonzalez-Aguilar J., Romero M., Steinfeld A., Stefanakos E., Goswami D.Y.: ***CRISPTower – A Solar Power Tower R&D Initiative in India***, ISES Solar World Congress, Cancun, Mexico, November 4-8, 2013.
- Good P., Zanganeh G., Ambrosetti G., Barbato M., Pedretti A., Steinfeld A.: ***Towards a Commercial Parabolic Trough CSP System Using Air as Heat Transfer Fluid***, Proc. 19th SolarPACES Conference, Las Vegas, NV, USA, September 17-20 (2013); doi:10.1016/j.egypro.2014.03.041, Energy Procedia **49**, 381–385 (2014).
- Guillot E., Alxneit I., Ballestrin J., Sans J.L., Willsh C.: ***Comparison of 3 Heat flux gauges and a water calorimeter for concentrated solar irradiance measurement***, Proc. 19th SolarPACES Conference, Las Vegas, NV, USA, September 17-20 (2013); doi:10.1016/j.egypro.2014.03.221, Energy Procedia **49**, 2090-2099 (2014).
- Haselbacher A., Stroehle S., Zanganeh G., Jovanovic Z., Steinfeld A.: ***An overview of high-temperature thermochemical and combined sensible/latent thermal energy storage***, 13th International Conference on Sustainable Energy Technologies, Geneva, Switzerland, August 25-28, 2014.
- E. Koepf, W. Villasmil, A. Meier: ***Demonstration of a 100-kWth High-Temperature Solar Thermochemical Reactor Pilot Plant for ZnO Dissociation***, Proc. 21st SolarPACES Conference, Cape Town, South Africa, October 13-16, 2015; to be published by AIP.
- Koepf E., Villasmil W., Meier A.: ***High temperature flow visualization and aerodynamic window protection of a 100-kWth solar thermochemical receiver-reactor for ZnO dissociation***, Proc. 20th SolarPACES Conference, Beijing, China, September 16-19, 2014; Energy Procedia **69**, 1780-1789, 2015.
- Marti J., Roesle M., Steinfeld A.: ***Combined experimental-numerical approach to determine radiation properties of particle suspensions***, Proc. ASME 2013 Summer Heat Transfer Conference, HT2013-17015, Minneapolis, USA, July 14-19, 2013.
- Neises-von Puttkamer M., Takacs M., Haueter P., Maier M., Steinfeld A.: ***Metal oxide reduction using a solar-driven vacuum thermogravimeter***, Proc. ASME 7th International Conference on Energy Sustainability, ES-FuelCell2013-18050, Minneapolis, USA, July 14-19, 2013.
- Pozivil P., Aga V., Zagorskiy A., Steinfeld. A.: ***A pressurized air receiver for solar-driven gas turbines***, Proc. 19th SolarPACES Conference, Las Vegas, USA, September 17-20, 2013.
- Scheffe J.R., Welte M., Steinfeld A.: ***Reduction of cerium dioxide in an aerosol tubular reactor for the thermal dissociation of CO2 and H2O***, Proc. ACS Annual Meeting, New Orleans, USA, April 7-11, 2013.
- Steinfeld A.: International Workshop "***Reaction Kinetics of Solar Thermochemical Redox Cycles***", Zurich, Switzerland, September 11, 2014.
- Stroehle S., Haselbacher A., Jovanovic Z., Steinfeld A.: ***One-dimensional Heat and Mass Transfer and discrete granule model of a tubular packed-bed reactor for thermochemical storage of solar energy***, Proc. ASME 2013 Summer Heat Transfer Conference, HT2013-17301, Minneapolis, USA, July 14-19, 2013.

- Villasmil W., Meier, Steinfeld A.: ***Dynamic modeling of a solar reactor for zinc oxide thermal dissociation and experimental validation using IR thermography***, Proc. ASME 2013 7th International Conference on Energy Sustainability, ES-FuelCell2013-18042, Minneapolis, MN, USA, July 14-19, 2013.
- Wirz M., Roesle M., Steinfeld A. **Design point for predicting year-round performance of solar parabolic trough concentrator systems**, Proc. ASME 7th International Conference on Energy Sustainability, ES-FuelCell2013-18055, Minneapolis, USA, July 14-19, 2013.
- Zanganeh G., Ambrosetti G., Pedretti A., Zavattoni S., Barbato M., Good P., Haselbacher A., Steinfeld A.: ***A 3 MWth parabolic trough CSP plant operating with air at up to 650°C***, IRSEC – 2nd International Renewable and Sustainable Energy Conference, Ouarzazate, Morocco, October 17-19, 2014.
- Zanganeh G., Pedretti A., Zavattoni S., Barbato M., Haselbacher A., Steinfeld A.: ***Design of a 100 MWh$_{th}$ Packed-bed Thermal Energy Storage***, Proc. 19th SolarPACES Conference, Las Vegas, NV, USA, September 17-20 (2013);
  doi: 10.1016/j.egypro.2014.03.116, Energy Procedia **49**, 1071–1077, 2014.
- Zavattoni S.A., Barbato M.C., Pedretti A., Zanganeh G., Steinfeld A.: ***High temperature rock-bed TES system suitable for industrial-scale CSP plant – CFD analysis under charge/discharge cyclic conditions***, IRES 2013 - 8th International Renewable Energy Storage Conference and Exhibition, Berlin, Germany, Nov. 18-20, 2013;
  doi: 10.1016/j.egypro.2014.01.165, Energy Procedia **46**, 124-133, 2014.

Invited Talks

- Alxneit I.: ***Solar Power Technologies Part I: Fundamentals***, Indian Institute of Chemical Technology (IICT) Hyderabad, India, June 17, 2013.
- Alxneit I.: ***Solar Power Technologies Part II: Solar Fuels***, Indian Institute of Chemical Technology (IICT) Hyderabad, India, June 18, 2013.
- Alxneit I.: ***Doped Ceria to Use in Thermochemical Cycles***, Indian Institute of Chemical Technology (IICT), Hyderabad, India, July 8, 2014.
- Alxneit I.: ***Temperature Measurement in Solar Furnaces and Solar Simulators***, Indian Institute of Chemical Technology (IICT), Hyderabad, India, July 9, 2014.
- Meier A.: ***Solar Thermal Electricity & Solar Thermochemical Fuels,*** SolarPACES Workshop “Roadmap to Solar Fuels”, Cypress Lakes, Hunter Valley, Australia, April 23, 2013.
- Meier A.: ***Solar Fuels – Coal & Gas Conversion,*** SolarPACES Workshop “Roadmap to Solar Fuels”, Cypress Lakes, Hunter Valley, Australia, April 23, 2013.
- Meier A.: ***Future Solar Fuels – H_2, Syngas, and Liquid Hydrocarbons,*** SolarPACES Workshop “Roadmap to Solar Fuels”, Cypress Lakes, Hunter Valley, Australia, April 23, 2013.
- Meier A.: ***Solar Minerals Processing – Fossil Fuel Displacement,*** SolarPACES Workshop “Roadmap to Solar Fuels”, Cypress Lakes, Hunter Valley, Australia, April 23, 2013.
- Meier A.: ***SolarPACES Task II – Solar Chemistry Research,*** SolarPACES Symposium, Newcastle, Australia, April 18, 2013.
- Meier A.: ***From Solar Power to Solar Fuels,*** SolarPACES Workshop “Roadmap to Solar Fuels”, Potchefstroom, South Africa, February 14-15, 2013.
- Meier A.: ***Solar Gasification of Carbonaceous Feedstock,*** SolarPACES Workshop “Roadmap to Solar Fuels”, Potchefstroom, South Africa, February 14-15, 2013.
- Meier A.: ***H_2, Syngas, and Liquid Fuels from H_2O, CO_2, and Sunlight,*** SolarPACES Workshop “Roadmap to Solar Fuels”, Potchefstroom, South Africa, February 14-15, 2013.
- Meier A.: ***Solar Production of Lime and Cement,*** SolarPACES Workshop “Roadmap to Solar Fuels”, Potchefstroom, South Africa, February 14-15, 2013.
- Meier A.: ***Thermochemical Energy Storage,*** SolarPACES Workshop “Roadmap to Solar Fuels”, Potchefstroom, South Africa, February 14-15, 2013.
- Meier A.: ***SolarPACES Initiative for a Solar Fuels Roadmap***, Plenary Session “Solar Fuels”, 20th SolarPACES Conference, Beijing, China, September 18, 2014.

- Meier A.: ***Solar Thermal Electricity & Solar Thermochemical Fuels***, Hybrid Solar/Fossil Energy Conference, Fossil Fuel Foundation, Johannesburg, South Africa, August 20-21, 2014.
- Meier A.: ***Solar-driven Gasification of Carbonaceous Feedstock***, Hybrid Solar/Fossil Energy Conference, Fossil Fuel Foundation, Johannesburg, South Africa, August 20-21, 2014.
- Meier A.: ***Solar Mineral Processing & Thermochemical Production***, Hybrid Solar/Fossil Energy Conference, Fossil Fuel Foundation, Johannesburg, South Africa, August 20-21, 2014.
- Meier A.: ***Future Solar Fuels – H2, Syngas, and Jet Fuels***, Hybrid Solar/Fossil Energy Conference, Fossil Fuel Foundation, Johannesburg, South Africa, August 20-21, 2014.
- Meier A.: ***Solar Thermal Electricity & Solar Thermochemical Fuels***, SolarPACES Workshop "Roadmap to Solar Fuels", Xi'an, China, December 10-11, 2015.
- Meier A.: ***Solar-driven Gasification of Carbonaceous Feedstock***, SolarPACES Workshop "Roadmap to Solar Fuels", Xi'an, China, December 10-11, 2015.
- Meier A.: ***Solar Processing of Minerals & Production of Chemicals***, SolarPACES Workshop "Roadmap to Solar Fuels", Xi'an, China, December 10-11, 2015.
- Meier A.: ***Solar Thermochemical Fuels – H_2, Syngas, and Liquid Fuels***, SolarPACES Workshop "Roadmap to Solar Fuels", Xi'an, China, December 10-11, 2015.
- Scheffe J., Steinfeld A.: ***Solar Thermochemical Splitting of H_2O and CO_2 using Metal Oxide Based Redox Cycles***, *IASS Workshop – Sustainable Fuels from Renewable Energies*, Potsdam, Germany, November 19, 2013.
- Steinfeld A.: ***Solar Thermochemical Processing of Fuels and Materials***, Keynote, 5th High Temperature Processing Symposium, Swinburne University of Technology, February 4, 2013.
- Steinfeld A.: ***Solar Mineral Processing***, Keynote, 1st Australian Workshop on Solar Thermal Chemical and Industrial Processes, University of Adelaide, February 8, 2013.
- Steinfeld A.: ***Solar thermochemical H2O and CO2 splitting utilizing a reticulated porous ceria redox system***, Keynote, Symposium on Porous Ceramics for CSP Applications, SUPSI, Lugano, June 26, 2013.
- Steinfeld A.: ***Solar thermochemical H2O and CO2 splitting utilizing a reticulated porous ceria redox system***, IBM Zurich Research Laboratory, July 1, 2013.
- Steinfeld A.: ***Novel Processes and Materials for Concentrated Solar Power and Thermochemical Fuel Production***, Keynote, International Solar Energy Society – Solar World Congress 2013, Cancun, Mexico, November 11, 2013.
- Steinfeld A.: ***Novel Processes and Materials for Concentrated Solar Power and Thermochemical Fuel Production***, Caltech – Chemical Engineering Seminar, November 14, 2013.
- Steinfeld A.: ***Solar thermochemical H_2O and CO_2 splitting utilizing a reticulated porous ceria redox system***, Universidad Rey Juan Carlos, Madrid, Spain, January 23, 2014.
- Steinfeld A.: ***Solar thermochemical gasification***, REPSOL Technological Center, Madrid, Spain, January 24, 2014.
- Steinfeld A.: ***Solar Syngas***, Solve-for-X, San Martin CA, USA, February 4, 2014.
- Steinfeld A.: ***Novel Processes and Materials for Concentrated Solar Power and Thermochemical Fuel Production***, University of Texas El Paso – Shell Energy Security and Climate Change Seminar, El Paso, TX, USA, February 10, 2014.
- Steinfeld A.: ***Novel Processes and Materials for Concentrated Solar Power and Thermochemical Fuel Production***, University of Arizona – Aerospace and Mechanical Engineering Seminar, Phoenix, AZ, USA, February13, 2014.
- Steinfeld A.: ***Solar Thermochemical Fuel Production via Metal Oxide Redox Cycles***, Berner Chemische Gesellschaft Seminar Series, University of Bern, May 7, 2014.
- Steinfeld A.: ***Kerosene from H2O, CO2, and Solar Energy***, 17. Kölner Sonnenkolloquium, Deutsches Zentrum für Luft- und Raumfahrt (DLR), Köln, Germany, June 5, 2014.
- Steinfeld A.: ***Technological Advances in Concentrated Solar Power***, Industry Day, ETH Zurich, August 26, 2014.
- Steinfeld A.: ***Solar Liquid Fuels from H2O and CO2***, Symposium Industrial High-temperature Solar Energy, Neuchâtel, November 6, 2014.

- Wieckert C.: ***Konzentrierte Solarenergie – Optionen für die zukünftige Energieversorgung***, Smart Grid Cycle, Villigen, May 28, 2013.
- Wieckert C.: ***Major material needs for the use of concentrated solar energy***, EERA JP-AMPEA Workshop “Materials for extreme operating conditions”, Espoo, Finland, June 2-3, 2013.
- Wieckert C.: ***High temperature furnaces heated by concentrated solar irradiation***, Jubiläumskolloquium 80 Jahre Elino Industrieofenbau GmbH, Düren, Germany, June 20, 2013.
- Wieckert C.: ***Thermal processing of Waelz oxide using concentrated solar energy***, GDMB Zinc Expert Meeting, Leoben, Austria, October 21-23, 2013.
- Wieckert C.: ***Solar thermochemical processing of solids using packed bed two-cavity reactors***, CSIRO, Newcastle, Australia, July 3, 2014.

References

[1] A. Meier: ***Solar Production of Zinc and Hydrogen – 100 kW Solar Pilot Reactor for ZnO Dissociation***, BFE Verfügung - Zusatz Nr. 2, Nr. SI/500403-01, 2013-2015.

[2] A. Meier, D. Gstöhl: ***Towards Industrial Solar Production of Zinc and Hydrogen – 100 kW Solar Pilot Reactor for ZnO Dissociation***, BFE Verfügung Nr. SI/500403-01, 2010-2011.

[3] A. Meier: ***Solar Production of Zinc and Hydrogen – 100 kW Solar Pilot Reactor for ZnO Dissociation***, BFE Verfügung - Zusatz Nr. 1, Nr. SI/500403-01, 2012-2013.

[4] A. Meier, A. Steinfeld: ***Solar Production of Zinc and Hydrogen – Reactor Optimization for Scale-Up***, BFE Verfügung Nr. SI/500108-01, 2008-2011.

[5] P. Loutzenhiser, A. Meier, A. Steinfeld, Review of the two-step H2O/CO2-splitting solar thermochemical cycle based on Zn/ZnO redox reactions, Materials 3, 4922-4938, 2010. http://dx.doi.org/10.3390/ma3114922

[6] A. Meier: ***Solar Production of Zinc and Hydrogen – 100 kW Solar Pilot Reactor for ZnO Dissociation***, BFE Project Nr. SI/500403-01, Annual Report, December 20, 2013.

[7] A. Meier: ***Solar Production of Zinc and Hydrogen – 100 kW Solar Pilot Reactor for ZnO Dissociation***, BFE Project Nr. SI/500403-01, Intermediate Report, July 23, 2014.

[8] W. Villasmil, M. Brkic, D. Wuillemin, A. Meier, A. Steinfeld: ***Pilot scale demonstration of a 100-kWth solar thermochemical plant for the thermal dissociation of ZnO***, ASME Journal of Solar Energy Engineering **136**, 011017-1/11, 2014. doi:10.1115/1.4025512

[9] Koepf E., Villasmil W., Meier A.: ***High temperature flow visualization and aerodynamic window protection of a 100-kWth solar thermochemical receiver-reactor for ZnO dissociation***, Energy Procedia **69**, 1780-1789, 2015. doi: 10.1016/j.egypro.2015.03.148

[10] J. Petrasch, P. Coray, A. Meier, M. Brack, P. Häberling, D. Wuillemin, A. Steinfeld, ***A novel 50 kW 11,000 suns high-flux solar simulator based on an array of xenon arc lamps***, J. Solar Energy Eng. **129**(4), 405-411, 2007. http://dx.doi.org/10.1115/1.2769701

[11] M. Kovacs: ***Optimizing the aerodynamic protection of a thermochemical-reactor window by high-temperature flow visualization and IR thermography***, Semester Thesis, PSI Villigen and ETH Zürich, May 2014.

[12] L. Schunk, A. Steinfeld: ***Kinetics of the thermal dissociation of ZnO exposed to concentrated solar irradiation using a solar-driven thermogravimeter in the 1800-2100 K range***, AIChE Journal **55**, 1497–504, 2009. http://dx.doi.org/10.1002/aic.11765

[13] E.E. Koepf, M.D. Lindemer, S.G. Advani, A.K. Prasad, ***Experimental Investigation of Vortex Flow in a Two-Chamber Solar Thermochemical Reactor***, J. Fluids Eng. **135**, 111103/1-12, 2013.

[14] I.M. Cohen, P.K. Kundu. Fluid Mechanics. Academic Press, 2004.

[15] MWSF, PROMES-CNRS, accessed 11 Dec 2012. http://www.promes.cnrs.fr/index.php?page=mega-watt-solar-furnace

[16] E. Koepf, W. Villasmil, A. Meier: ***Demonstration of a 100-kWth High-Temperature Solar Thermochemical Reactor Pilot Plant for ZnO Dissociation***, Proc. 21st SolarPACES Conference, Cape Town, South Africa, October 13-16, 2015; to be published by AIP.

[17] W. Villasmil: ***Dynamic Modeling and Experimental Demonstration of a 100-kW$_{th}$ Solar Thermochemical Reactor for ZnO Dissociation***, PhD Thesis Nr. 21675, ETH Zürich, December 2013. http://e-collection.library.ethz.ch/view/eth:8161

[18] W. Villasmil, A. Meier, A. Steinfeld: ***Dynamic modeling of a solar reactor for zinc oxide thermal dissociation and experimental validation using IR thermography***, ASME Journal of Solar Energy Engineering **136**, 011015-1/11, 2014. doi:10.1115/1.4025511

[19] R. Jakober: ***Technoeconomic Analysis of an Industrial Plant for H_2 Production via the Zn/ZnO Solar Thermochemical Cycle***, Master Thesis, PSI Villigen and ETH Zürich, February 2015.